Integration of offshore energy into national energy system: a case study on Belgium

Jocelyn Mbenoun[a], Amina Benzerga[a], Bardhyl Miftari[a], Ghislain Detienne[b], Thierry Deschuyteneer[b], Juan Vazquez[b], Guillaume Derval[a,*], Damien Ernst[a,c]

[a] *Montefiore Institute, Liège, Belgium*
[b] *Fluxys*
[c] *LTCI, Télécom Paris, Institut Polytechnique de Paris, France*

Abstract

Offshore wind farms are typically connected to the mainland via HVAC or HVDC lines. Another possibility to transmit energy is using molecules instead of electricity which may lead to reduced cost and better storage opportunities. This paper proposes a multi-carrier (natural gas, electricity and hydrogen) model of the Belgium energy system in 2050, under carbon neutrality constraint, to assess whether an energy mix should contain offshore hydrogen production. While HV lines remain the main way of transmitting energy from the offshore farm to mainland, the results show that depending on the renewable capacities, the distance between the wind farm and the coast, and the price of hydrogen import, producing H_2 offshore could be beneficial.

Keywords: Graph-based optimisation modelling language, energetic system modelling, offshore hub, hydrogen, multi-energy system.

1. Introduction

The European Commission has targeted carbon neutrality in EU27 by 2050. In this regard, several scenarios have been proposed to reach the set targets by different actors, such as academics, industries, TSO of gas and electricity[1, 2, 3, 4]. All these scenarios stress the importance of increasing renewable energy production. The same applies for the Belgium energy transition which possesses a moderate but not yet reached potential in offshore wind energy and still have room to increase its onshore wind and solar PV energy production [5].

Another part of the solution to achieve carbon neutrality is the decarbonisation of certain sectors, especially the heating, transport, and industry sectors. One of the fastest ways it could be achieved is through electrification. Electric vehicles and heat pumps are already mature technologies and are more efficient than their fossil fuels and gas-fueled counterparts [6]. Moreover, both can be used as short-term storage and demand-shifting potential. In the industry sector, electricity can also be used as a source of energy for low-temperature (e.g. heat pump), medium-temperature (e.g. electric infrared heating) or high-temperature (e.g. induction heating, electric arc furnace) heating processes [7].

*Corresponding author.
Email addresses: jmbenoun@uliege.be (Jocelyn Mbenoun), abenzerga@uliege.be (Amina Benzerga), bmiftari@uliege.be (Bardhyl Miftari), ghislain.detienne@fluxys.com (Ghislain Detienne), thierry.deschuyteneer@fluxys.com (Thierry Deschuyteneer), juan.vazquez@fluxys.com (Juan Vazquez), gderval@uliege.be (Guillaume Derval), dernst@uliege.be (Damien Ernst)

In this aspect, the Belgium transmission system operator (TSO) Elia has laid plans to develop the Belgian power grid in order to make it ready to cope with the increase in electricity production and consumption [8]. For the development of the high-voltage grid (380 kV), three pillars were identified:

- the development of the offshore network to bundle the connections of additional offshore wind farms and to ensure economically efficient transmission to the land,
- the reinforcement and the extension of interconnection capacity with adjacent countries,
- the reinforcement and extension of the power grid within Belgium.

However, it comes with substantial costs in electrical infrastructure [9].

A solution to mitigate these costs could be to support the decarbonisation by electrification with the use of green molecules (green or blue hydrogen and synthetic methane). Hydrogen is already used as feedstock for iron, steel, ammonia, fuel production and the petrochemical industry, but it is mainly produced through steam methane reforming (SMR) which releases carbon dioxide. Blue hydrogen (connecting a carbon capture unit to the SMR device) or green hydrogen (produced from electrolyser using green electricity) could be used as feedstock instead. Hydrogen can also partially substitute the current use of natural gas for medium and high-temperature processes, as well as its use in power plants and can also be used as fuel for transport [10]. Synthetic methane can also be used as a substitute for natural gas. It does not require any adaptation from the existing gas network and can be easily stored. Part of the gas network can also be repurposed in order to deliver hydrogen, decreasing the cost of supply of this latter molecule [10]. However, both hydrogen and synthetic methane require specific and expensive infrastructure to be produced. Furthermore, the use of green molecules increases the total energy demand due to the conversion losses during their production [6]. This is the reason why the energy demand in futuristic scenarios assumes a partial electrification for certain sectors and the other part is decarbonized via the consumption of green molecules [1, 6]. Those scenarios differ in the proportion of green electrons vs green molecules consumed.

This paper aims to challenge the first pillar of the development of the high-voltage grid according to Elia, more specifically the interconnection between offshore wind farms and inland Belgium. It aims to explore whether transporting a portion of the energy generated by offshore wind turbines to mainland Belgium in the form of green hydrogen or synthetic methane would be more advantageous, rather than solely relying on electricity. To this end, an integrated energy system model divided in three geographical regions called clusters, the offshore hub, the coastal area and the Belgium inland, is designed. The objective of this division is to correctly assess the quantity of energy transferred from the offshore hub to inland Belgium and, as a result, the type of infrastructure needed to transport this energy. The modelling of inland Belgium draws inspiration from the optimisation model created in [11]. This model comprises a wide range of technologies and considers the three energy carriers used to supply energy from the offshore hub (electricity, hydrogen and natural gas/methane) and one additional commodity, the carbon dioxide. The energy demands consider different sectors and scenarios from the 2022 TYNDP of ENTSO-E and ENTSOG are used for their annual values [1]. A strong constraint of the model is to reach carbon neutrality with scenarios for the year 2050.

The remainder of this paper is organised as follows. Section 2 reviews related works about integrated energy systems and offshore and remote hubs and highlights the areas to which the present paper contributes. Section 3 discusses the assumptions and features of the model, presents the modelling language used and describes the model formulation. Section 4 introduces the case studies that will be analysed in Section 5. Section 6 propose sensitivity analyses and Section 7 describe the limitations of the model.

2. Related works

This paper is related to three bodies of work: integrated energy systems, optimisation tools and integration of offshore energy.

Integrated energy systems are widely used to model and evaluate potential pathways toward carbon emission neutrality. These integrated systems can be viewed as networks of interconnected units or components [12], comprising different energy carriers and are described as planning and control problems. On the one hand, planning problems are concerned with the optimal design of a certain system, e.g. finding the optimal investment or macro-level decisions to produce a given amount of energy. On the other hand, control problems try to optimally operate a given already-designed system to achieve a certain goal. Planning and control problems try to both design and operate a system to attain a certain goal (objective). For instance, finding the optimal battery and PV capacities to minimise the overall bill in a microgrid [13].

A common way of tackling these problems is mathematical programming, in particular Mixed-Integer Linear Programming (MILP) [14] or Linear Programming (LP) [15]. In mathematical programming, the problems are formulated using variables, constraints and an objective function to optimise. In LP, we consider the constraints and the objective function affine and the variables continuous. In MILP, we also consider integer and binary variables. MILP and LP enable users to deal with large problems while still taking into account the operational constraints of each unit and each interconnection. Different tools can be used to formulate and solve those problems. A comparison of those different tools has been made in [16]. The key elements in this comparison was the fact that these tools could be divided into two classes : Algebraic modelling languages (AMLs) such as AMPL [17] or Pyomo [18] and object-oriented modelling environments (OOMEs) such as PyPSA [19] or Calliope [20]. GBOML is a hybrid modelling tool, in-between AMLs and OOMEs. GBOML enables one to encode structure, define templates of technologies, allows reuse and model assembling, i.e. key features that are particularly useful for modelling wide energy systems and enabling their extension. It furthermore has a formulation close to the mathematical one and can encode any MILP.

A comprehensive evaluation of integrated energy systems is provided in [21], offering a critical overview of models and evaluation methodologies aimed at analysing multi-energy systems. These methodologies encompass notions such as energy hubs and microgrids. Additionally, [22] proposes a methodology for the simultaneous optimisation of energy systems involving multiple energy carriers, including electricity, natural gas, and district heating. Authors in [23] survey notable methodologies employed to capture the repercussions of variability in power systems within integrated system models. These methodologies consider temporal aspects and employ simplifying assumptions to render the computational handling of such models feasible. One of these methodologies is implemented in [24], where an innovative operational model encompassing both electrical and gas systems is introduced.

Within the Belgian context, similar studies have been done. For instance, [11] proposes an integrated system that evaluates the potential of sector coupling through power-to-gas and carbon capture technologies to achieve ambitious decarbonization targets, involving electricity, hydrogen, natural gas, synthetic methane, and carbon dioxide. Limpens et al. [3] present an exhaustive energy system encompassing 94

technologies and 24 resources, which are tasked with providing hourly provisions for heating, electricity, transportation, and non-energy demands. Furthermore, a collaborative technical report by the "Federal Planning Bureau", the "Vlaams Instituut voor Technologisch Onderzoek," and the "Institut de Conseil et d'Études en Développement Durable" scrutinizes the feasibility and ramifications of transforming the Belgian energy system into a 100% renewable energy paradigm [4]. While all of these models offer valuable insights into potential pathways for Belgium's energy transition, none of them explore the option of producing hydrogen directly offshore and then transporting it to the shore in that form.

However, the big challenge that comes with large investments in offshore wind power mainly concerns how to smoothly fit the generated electricity into current energy systems. Indeed, wind electricity generation is intermittent and consequently, it does not align with the patterns of the electricity demand. Furthermore, offshore wind generation requires massive grid reinforcements [25]. In this context, green hydrogen produced from offshore wind emerges as a promising solution to overcome these obstacles.

Various studies have been carried out to assess the potential benefits of offshore energy hubs that produce hydrogen or other electrofuels directly on-site. The study in [26] introduces a model proposing an integrated design for hydrogen and offshore electric power infrastructure, thereby determining the levelised costs of both hydrogen and electricity. Similar studies have been done in [27] and [28] which focus on the supply of wind hydrogen based on variables such as electrolyser technology, floating wind platforms, and energy transmission vectors. Another possibility such as the production of electrofuel from wind electricity is emphasised in [29] to export renewable fuels to sectors historically characterised by high greenhouse gas emissions. All these studies propose a techno-economical study where costs for molecules or electrons are assessed but do not consider the integration of the offshore production in an inland energy system. The literature is still missing models that connect a multi-energy offshore hub with a comprehensive inland energy system. This gap is notable because such an interconnection could lead to unforeseen dynamics, not only between the offshore hub and the inland energy system but also in the production of various energy carriers within the model.

In this paper, the objective is to associate a comprehensive Belgium energy system comprising a wide variety of technologies generating electricity, hydrogen and methane and an offshore energy hub producing electricity and green hydrogen. Based on [23], an hourly granularity is considered to capture the intermittence of renewable energy generation. The investment and the dispatch are co-optimised for an entire year and an open-source modelling framework is described.

3. Methodology

This section discusses the modelling language used, namely GBOML, the main assumptions of the model, and presents its mathematical description.

3.1. GBOML

In this paper, the Graph-Based optimisation Modelling Language (GBOML version 0.1.7), an open-source software developed at the University of Liège [16], is used to model the energy system. This language enables one to describe an optimisation problem as a hierarchical hypergraph composed of nodes connected by hyperedges. Each node can be seen as an optimisation sub-problem with its own sets of parameters, variables, constraints, local objectives and its own sub-hypergraph. Constraints composed of variables from different nodes can then be defined in a hyperedge to connect different nodes. A detailed mathematical formulation of the GBOML framework is described in Section 3 of [30].

3.2. Mathematical formulation

The mathematical formulation of the energy system in this paper is inspired by [12] where a practical application of GBOML to energy supply chains is described. Nodes typically represent a technology or a process while hyperedges may be used to enforce some coupling between plants. The same principles apply in this paper. Generic nodes model five types of technologies or processes: conversion nodes, flexibility nodes, import/export nodes, transmission nodes and demand nodes. A sixth type, referred to as a cluster, will be a node comprising its own sub-hypergraph (i.e., its own set of nodes and hyperedges). Hyperedges connect nodes and clusters producing/importing or consuming/exporting the same commodity and ensure the balance of flow for each commodity. A global discretised time horizon $T \in \mathbb{N}$ and associated set of time periods $\mathcal{T} = \{0, 1, ..., T - 1\}$ common to all nodes, are also defined. Similar to [12], parameters are written in Greek letters, sizing variables in capital Latin letters and operation variables in lowercase Latin letters.

3.2.1. Modelling assumptions

The model is based on four central assumptions:

Central planning and operation.. A single entity makes investment and dispatch decisions with the aim of minimising total system cost.

Perfect foresight and knowledge.. The entity designing and operating the system has complete knowledge and foresight, thus all technical and economic aspects as well as anticipated weather events and demand patterns are considered as known.

Investment and operational decisions.. Investment decisions are made at the start of the time horizon, and assets are immediately available, according to a static investment model. Hourly time steps are used to make operational decisions. Operational and investment decisions are co-optimised in a unique LP problem. Consequently, no market system is considered.

Technology and process models.. A set of affine input-output relations that typically express mass and energy balances at the plant or process level are used to model the sizing and operation of technologies. Only storage systems provide a straightforward state space representation, whereas some technologies take into account input or output dynamics.

There are many other assumptions mostly linked to how some technologies are modelled. These are described in the next sections. Of course, all these assumptions induce limitations that will be described in section 7.

3.2.2. Conversion nodes

Conversion nodes refer to nodes carrying out the conversion of a set of commodities to another via a technology or a process. Let $n \in \mathcal{N}$ be a conversion node, commodity flows are modelled as variables, and an index $i \in \mathcal{I}^n$ is assigned to each commodity. Let $q^n_{r,t}$ be the flow of the reference commodity $r \in \mathcal{I}^n$ at time t of node n, the flow of all other commodities $q^n_{i,t}$ $\forall i \in \mathcal{I}^n \setminus \{r\}$ of node n is modelled via a set of linear equations which read:

$$q^n_{r,t} = \phi^n_i q^n_{i,t} \qquad \forall i \in \mathcal{I}^n \setminus \{r\},\ \forall t \in \mathcal{T} \tag{1}$$

where $\phi^n_i \in \mathbb{R}_+$ is the *conversion factor* between commodity r and i (for example in a gas power plant, the commodity r is the electricity produced and i is the gas consumed). The maximum flow of a reference commodity r is limited by the flow capacity K^n of the technology n such that:

$$q^n_{r,t} \leq \pi^n_t K^n \qquad \forall t \in \mathcal{T}. \tag{2}$$

$\pi^n_t \in [0,1]$ indicates the maximum production per capacity of technology n at time t; it is typically used to represent exogenous factors such as solar irradiation and wind. The flow capacity K^n is a variable and may be bounded using the constraint:

$$\underline{\kappa}^n \leq K^n \leq \bar{\kappa^n}, \tag{3}$$

where $\underline{\kappa}^n \in \mathbb{R}_+$ represents the existing capacity and $\bar{\kappa}^n \in \mathbb{R}_+$ the maximum capacity of technology n that may be installed. Various operational limitations can also be taken into account. For example, certain conversion technologies may have specific operating ranges and require a minimum flow of commodity $r \in \mathcal{I}^n$ to be maintained in order to function properly. If $\mu^n \in [0,1]$ represents the minimum operating level (as a fraction of the installed capacity), this requirement can be expressed as:

$$\mu^n K^n \leq q^n_{r,t} \qquad \forall t \in \mathcal{T}. \tag{4}$$

There may also be restrictions on how quickly the flow of commodity $r \in I^n$ can change, which are known as ramping constraints and expressed as:

$$q^n_{r,t} - q^n_{r,t-1} \leq \Delta^n_{r,+} K^n \qquad q^n_{r,t} - q^n_{r,t-1} \geq -\Delta^n_{r,-} K^n \qquad \forall t \in \mathcal{T} \setminus \{0\}, \tag{5}$$

with $\Delta^n_{r,+} \in [0,1]$ and $\Delta^n_{r,-} \in [0,1]$ are the maximum rates at which flows can be ramped up and down (as a fraction of the installed capacity per unit time), respectively.

Certain technologies are susceptible to planned outages, which can influence their yearly availability.

To address this consideration, a new parameter denoted as $\alpha^n \in [0,1]$ is introduced. This parameter represents the proportion of time within a year, expressed as a percentage, during which outages are assumed to occur for technology n, respectively:

$$\sum_{t\in\mathcal{T}} q^n_{r,t} \leq (1-\alpha^n) \sum_{t\in\mathcal{T}} K^n \qquad \forall t \in \mathcal{T}. \tag{6}$$

The model can then optimally divide these outages when they have the least impact.

For some nodes, the total amount of their reference commodity is limited by the equation:

$$\sum_{t\in\mathcal{T}} q^n_{r,t} \leq \nu \kappa^n_{tot} \tag{7}$$

where $\nu \in \mathbb{N}$ is the number of years spanned by the optimisation horizon and κ^n_{tot} is the annual amount of commodity r that can be produced by node n (for example, the amount of biomass may be limited).

A cost function must be minimised. This function takes into account the investment, the maintenance and the operation as follows:

$$F^n = \nu(\zeta^n + \theta^n_f)(K^n - \underline{\kappa}^n) + \sum_{t\in\mathcal{T}} \theta^n_v q^n_{r,t} \delta t, \tag{8}$$

where $\nu \in \mathbb{N}$ is the number of years spanned by the optimisation horizon, $\zeta^n \in \mathbb{R}_+$ represents the annualised investment cost, $\theta^n_f \in \mathbb{R}_+$ models fixed operation and maintenance (FOM) costs and $\theta^n_v \in \mathbb{R}_+$ represents variable operation and maintenance (VOM) costs. The annualised investment cost is computed as follows:

$$\zeta^n = CAPEX^n \times \frac{w^n}{1-(1+w^n)^{-L^n}} \tag{9}$$

where $CAPEX^n$ is the capital expenditure, w^n is the weighted average cost of capital (WACC) and L^n is the lifetime of node n.

For certain nodes, a cost function related to an exogenous commodity consumed by some technologies (e.g. nuclear power plant) can also be added to the objective to minimise:

$$F^n_i = \chi^n_i \sum_{t\in\mathcal{T}} q^n_{i,t} \delta t \tag{10}$$

where $\chi^n_i \in \mathbb{R}_+$ is the cost of the commodity i consumed by the node n and $\delta t \in \mathbb{R}_+$ is the duration of each time period.

3.2.3. Flexibility nodes

A flexibility node plays a crucial role in maintaining equilibrium between production and demand. These nodes encompass various technologies including storage systems, linepack, and demand-side response mechanisms such as load shedding and load shifting. Load shedding refers to the capability of reducing a portion of the electrical demand at a very high price, while load shifting refers to the ability to delay a portion of the demand. Let $n \in \mathcal{N}$ be a *flexibility node*, let $e^n_t \in \mathbb{R}_+$ be the inventory level at

time t of node n, the inventory level dynamics is expressed by the equation:

$$e^n_{t+1} = (1 - \eta^n_S)e^n_t + \eta^n_+ q^n_{i,t} - \frac{1}{\eta^n_-} q^n_{j,t}, \qquad \forall t \in \mathcal{T} \setminus \{T-1\}, \tag{11}$$

where $q^n_{i,t}$ and $q^n_{j,t} \in \mathbb{R}_+$ represent commodity in- and out-flows at time t, respectively. $\eta^n_S \in [0,1]$ is the self-discharge rate per unit of time, $\eta^n_+ \in [0,1]$ is the charge efficiency and $\eta^n_- \in [0,1]$ is the discharge efficiency. The maximum inventory level is limited by the stock capacity of the technology $E^n \in \mathbb{R}_+$ modelled as a variable which may be bounded such that:

$$\underline{\epsilon^n} \leq E^n \leq \overline{\epsilon^n} \qquad e^n_t \leq E^n \qquad \forall t \in \mathcal{T} \tag{12}$$

where $\underline{\epsilon}^n$ represents the existing stock capacity and $\bar{\epsilon}^n$ represents the maximum stock capacity that can be installed; The commodity in- and out-flows are limited by the flow capacity of the technology K^n such that:

$$q_{i,t} \leq \rho^n K^n, \qquad q_{j,t} \leq K^n, \qquad \forall t \in \mathcal{T} \tag{13}$$

where $\rho^n \in \mathbb{R}_+$ represents the maximum charge-to-discharge ratio. The charge-to-discharge ratio is used when the maximum commodity in- and out-flows are asymmetric. K^n may be bound using either the constraint (3) or can be dependent on the stock capacity such that:

$$K^n = \xi^n E^n \tag{14}$$

where $\xi \in [0,1]$ is the flow-to-stock ratio capacity of node n.

To avoid edge effects at the last time step of the optimisation in storage operation, the inventory level at the first time step (i.e for $t = 0$), e^n_0 is constrained as:

$$e^n_0 = (1 - \eta^n_S)e^n_{T-1} + \eta^n_+ q^n_{i,T-1} + \frac{1}{\eta^n_-} q^n_{j,T-1}. \tag{15}$$

where $q^n_{i,T-1}$ and $q^n_{j,T-1}$ are in the commodity in- and out-flows at the last time step of the optimisation $t = T-1$.

The process of charging a storage system can involve the utilisation of another commodity, represented by $l \in \mathcal{I}^n, l \neq i, j$ (for example, electricity consumed by compressors). This dependency is incorporated into the model through an additional variable $q^n_{l,t} \in \mathbb{R}_+$ and the corresponding equation:

$$q^n_{l,t} = \phi^n_i q^n_{i,t}, \ \forall t \in \mathcal{T}. \tag{16}$$

Similar to conversion nodes, new equations are introduced to consider the planned outages of the technology n with:

$$\sum_{t\in\mathcal{T}} q^n_{i,t} \leq (1-\alpha^n)\sum_{t\in\mathcal{T}} K^n \qquad \forall t \in \mathcal{T} \tag{17}$$

$$\sum_{t\in\mathcal{T}} q^n_{j,t} \leq (1-\alpha^n)\rho^n\sum_{t\in\mathcal{T}} K^n \qquad \forall t \in \mathcal{T} \tag{18}$$

where $\rho^n \in \mathcal{R}_+$ represents the maximum discharge-to-charge ratio.

Load shifting and linepack can be seen as a storage technology with an obligation to be refilled at a specific hour of the day. Let $\mathcal{T}_D$ be the set of first time periods of every day in the optimisation horizon, $\gamma^n \in$ [0,23] be the hour of the day at which the node n must be refilled then the constraint forcing node n to be refilled is given by:

$$e^n_{h+\gamma^n} = E^n \qquad \forall h \in \mathcal{T}_D \tag{19}$$

Moreover, for load shifting and linepack, the amount of commodity that can be discharged during a day cannot exceed the amount of the quantity stored at the hour of refill. In other words, only one cycle of charge and discharge is allowed by day. This is modelled by limiting the daily amount of energy discharged using the constraint:

$$\sum_{t=0}^{23} q^n_{j,h+\gamma^n+t} \leq E^n \qquad \forall h \in \mathcal{T}_D. \tag{20}$$

Finally, for load shedding, it can be mathematically expressed as a "discharge flow" of commodity i. The quantity of commodity i that can be shed is also limited using:

$$\sum_{t=0}^{23} q^n_{i,h+t} \leq K^n\omega^n \qquad \forall h \in \mathcal{T}_D \tag{21}$$

where ω^n is a parameter representing the number of hours by day the load of node n can be shed at its maximum flow capacity. The cost function of the flexibility node nn to minimise is defined as [12]:

$$F^n = \left[\nu(\varsigma^n + \vartheta^n_f)(E^n - \underline{\epsilon}^n) + \sum_{t\in\mathcal{T}} \vartheta^n_v e^n_t \delta t\right] + \left[\nu(\zeta^n + \theta^n_f)(K^n - \underline{\kappa}^n) + \sum_{t\in\mathcal{T}} \theta^n_v q^n_{i,t}\delta t\right] \tag{22}$$

$\varsigma^n \in \mathbb{R}_+$ and $\zeta^n \in \mathbb{R}_+$ represent the stock and flow components of annual investment costs, $\vartheta^n_f \in \mathbb{R}_+$ and $\theta^n_f \in \mathbb{R}_+$ model the stock and flow components of FOM costs, while $\vartheta^n_v \in \mathbb{R}_+$ and $\theta^n_v \in \mathbb{R}_+$ represent the stock and flow components of VOM costs. ς^n and ζ^n are computed using Equation (9) with CAPEX for the stock and the flow components.

3.2.4. Import and export nodes

A node n is an *import node* or *export node* if it imports or exports a commodity i. Let $\underline{\kappa}^n_t \in \mathbb{R}_+$ be the existing flow capacity of node n at each time t (based on the capacity of a pipeline of gas, which

will constant, or the amount of renewable energy produced elsewhere, which would be a time series, for example), then the flow of commodity i from the import or export node n is limited with:

$$q^n_{i,t} \leq \underline{\kappa}^n_t \qquad \forall t \in \mathcal{T} \tag{23}$$

Unlike for conversion or flexibility nodes, the model is not allowed to invest in additional import or export capacities. The cost related to the imports/exports to minimise is given by:

$$F^n = \sum_{t \in \mathcal{T}} \sigma^n_t q^n_{i,t} \delta t \tag{24}$$

where σ^n_t is the cost of import or export of commodity i at time t for node n.

3.2.5. Transmission nodes

Transmission nodes comprise electrical lines, natural gas pipelines and hydrogen pipelines. For each transmission node, two directions are defined, the *forward* and *reverse*. Let $n \in \mathcal{N}$ be a transmission node, let $i \in \mathcal{I}^n$ and $j \in \mathcal{I}^n$ be the indices of the in/outflows of the commodity transported by node n, then the equations governing the transport of the commodity by technology n in the forward direction, indexed f, are:

$$q^n_{i_f,t} \leq K^n \qquad q^n_{j_f,t} = \phi^n_i q^n_{i_f,t} \qquad \forall t \in \mathcal{T} \tag{25}$$

$q^n_{i_f,t}$ and $q^n_{j_f,t} \in \mathbb{R}_+$ are the inflow and outflow of the commodity at time t and $K^n \in \mathbb{R}_+$ is the flow capacity. $\phi^n_i \in [0,1]$ is the loss factor accounting for the losses in the transmission node. Similar to conversion and flexibility nodes, the maximum capacity of a transmission node may be bounded,

$$\underline{\kappa}^n \leq K^n \leq \overline{\kappa}^n, \tag{26}$$

where $\overline{\kappa}^n$ is the maximum capacity of technology n that may be installed. The same equations constraint the flow of commodity in the reverse direction,

$$q^n_{i_r,t} \leq K^n \qquad q^n_{j_r,t} = \phi^n_i q^n_{i_r,t} \qquad \forall t \in \mathcal{T} \tag{27}$$

in which the suffix r instead of the suffix f stands for reverse direction. Similar to the process of charging a storage system, the flow of a commodity can involve the utilisation of another commodity, represented by $l \in \mathcal{I}^n, l \neq i, j$ (for example, electricity consumed by compressors). This dependency is incorporated into the model through an additional variable $q^n_{l,t} \in \mathbb{R}_+$ and the corresponding equation:

$$q^n_{l,t} = \phi^n_l (q^n_{i_f,t} + q^n_{i_r,t}), \ \forall t \in \mathcal{T}. \tag{28}$$

The cost function of the transmission node n to minimise is given by:

$$F^n = \nu(\zeta^n + \theta^n)(K^n - \underline{\kappa}^n) + \sum_{t \in \mathcal{T}} \theta^n_v (q^n_{i_f,t} + q^n_{i_r,t}) \delta t \tag{29}$$

where $\zeta^n \in \mathbb{R}_+$ is the annualised investment cost, $\theta^n_f \in \mathbb{R}_+$ models fixed operation and maintenance (FOM) costs and $\theta^n_v \in \mathbb{R}_+$ represents variable operation and maintenance (VOM) costs.

3.2.6. Demand nodes

A demand node consists of various time-series data used to model the demand across different sectors for a specific commodity i. Let $n \in \mathcal{N}$ be a demand node, $\lambda^n_{i,s,t}$ be the end user demand for commodity i from time-series s at time t, then $d^n_{i,t}$, the aggregated demand for commodity i at time t, is computed using:

$$d^n_{i,t} = \sum_{s \in \mathcal{S}^n_i} \lambda^n_{i,s,t} - l^n_{i,t} \qquad \forall t \in \mathcal{T} \tag{30}$$

where $\mathcal{S}^n_i$ is the set of all time-series considered for the demand of commodity i and $l^n_{i,t}$ is the energy not served for commodity i at time t. In this model, it is important to note that the electricity demand $g^n_{el,EV,t}$ generated by electric vehicles (EV) is not entirely external. Rather, the model assumes that the timing and intensity of EV charging can be strategically adjusted throughout the day. However, this optimisation is subject to the constraint that a certain daily supply level must be ensured with:

$$\sum_{t=0}^{23} g^n_{el,h+t} = \lambda^n_{el,EV,h} \qquad \forall h \in \mathcal{T}_D. \tag{31}$$

Subsequently, the aggregated demand for electricity at time t for the node comprising the demand for EV is given by:

$$d^n_{el,t} = \sum_{s \in \mathcal{S}^n_{el} \setminus \{EV\}} \lambda^n_{el,s,t} + g^n_{el,t} - l^n_{el,t} \qquad \forall t \in \mathcal{T} \tag{32}$$

The cost function of the node to minimise is:

$$F^n = \sum_{t \in \mathcal{T}} \sigma^n_t l^n_{i,t} \delta t. \tag{33}$$

σ^n_t being the cost associated with each quantity of energy not served.

3.2.7. Conservation hyperedges

As stated previously, hyperedges connect nodes and clusters producing/importing or consuming/exporting the same commodity and ensure the balance of flows for each commodity. Some of these flows are also limited by an interconnect capacity; this constraint is added to the hyperedges if needed.

4. Case Study

The section discusses the objective of the case study, provides a detailed description of the energy system and the different hypotheses made for each of the technologies.

4.1. Objective

The primary goal of this case study is to evaluate the capacity of renewable-based power generation, carbon capture, and sector coupling technologies to accomplish cross-sector decarbonization goals for the year 2050 at least cost. An in-depth analysis will be conducted, with particular emphasis on examining the potential advantages of domestic production in the context of competing with the importation of green hydrogen. Moreover, the optimal method for transporting energy to shore will be evaluated, considering whether it should be in the form of molecules (such as hydrogen) or electrons (such as electricity). This assessment will take into account various factors, including transmission efficiency, infrastructure costs, storage requirements, and energy demand patterns, to determine the most cost-effective approach for meeting energy demand.

To be able to reach those objectives, a model of the Belgium energy system is developed. The Belgium energy system is split into three distinct geographical regions represented as clusters in the model: the offshore areas (BE-OFF), a transit zone (BE-COA) and the inland Belgium (BE-INL). The energy demand needs to be satisfied across three energy carriers: electricity, natural gas, and hydrogen. Additionally, the carbon dioxide generated to fulfil these demands is taken into account and can be captured and exported.

This section follows a bottom-up approach to describe the model. It starts by introducing each type of node, followed by an explanation of how these nodes are incorporated into clusters, along with the hyperedges connecting them, forming the full model.

4.2. Nodes

A uniform WACC of 7% is assumed for all technologies, which corresponds to a situation in which the necessary funds to support the system are obtained through borrowing from capital markets. For nodes producing or importing hydrogen or methane, the parameters in GW or GWh are given for their low heating value (LHV).

4.2.1. Conversion nodes

Conversion nodes comprise solar panels (PV), onshore wind turbines (WON) and offshore wind turbines (WOFF), nuclear power plants (NK), fuel cells (FC), electrolyser plants (EP), desalination units (DU), methanation plants (MT), direct air capture units (DAC) and biomethane plants (BMT), combined cycle and open cycle gas turbines (CCGT and OCGT respectively), steam methane reformers (SMR) and post combustion carbon capture units (PCCC). Each of them is modelled with one variable representing the plant capacity and remaining variables representing different commodity in- and out-flows. Figure 1 displays the icons designated for representing each conversion node, along with the corresponding commodities consumed and produced by each of these nodes.

Equations (1 - 6), with π_t^n being either a time series for intermittent renewable technologies, or equal to 1 for all $t \in \mathcal{T}$ for dispatchable technologies in Equation (2), and the cost function (8) are used to

model those technologies. For biomethane plants, Equation (7) limiting its annual production is also used. The annual potential of biomethane produced is based on a study from Valbiom [31]. For NK and BMT, the cost function (10) is also added to consider the fuel cost.

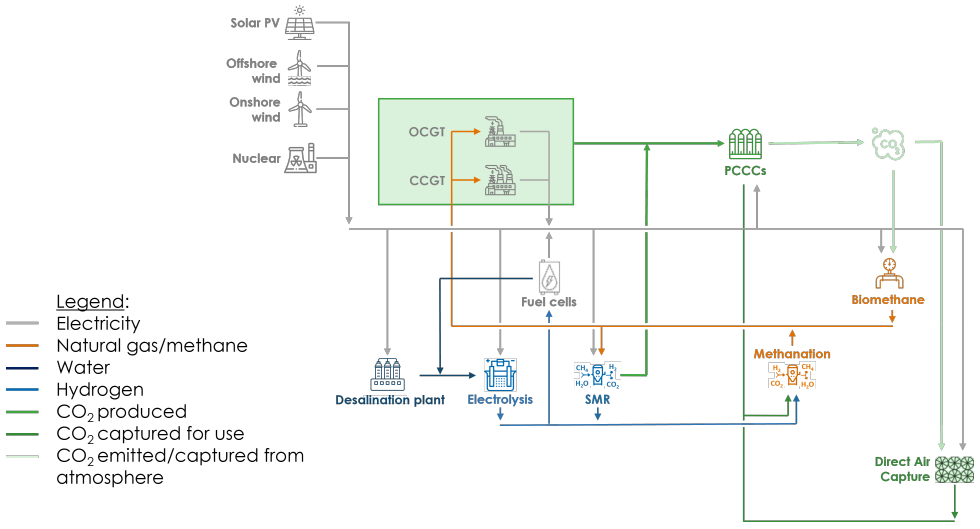

Figure 1: Representations of all conversion nodes with their produced and consumed commodities.

Three hypothetical commodities are used to represent carbon dioxide. $CO_{2,g}$ represents carbon dioxide in exhaust gas from combustion processes, $CO_{2,c}$ represents carbon dioxide captured for export or reuse, and $CO_{2,a}$ represents carbon dioxide in the atmosphere. Each unit of $CO_{2,g}$ can either be released into the atmosphere or captured by PCCC units. In these PCCC units, it is assumed that a maximum of 90% of the $CO_{2,g}$ is captured, while the remaining CO_2 is released into the atmosphere.

Technical and economic parameters of all the conversion nodes are presented in Tables 7, 8 and 9 in the Appendix. Almost all parameters are predictions for 2050 from several sources [32, 33, 34]. The parameters for both post-combustion carbon capture and desalination units are predictions for 2030 due to a lack of information for 2050 [11, 12].

4.2.2. Flexibility nodes (Storage, Demand-side response (DSR))

Storage. Storage technologies comprise the electrical battery (BAT), pumped-storage hydroelectricity (PHP), methane underground storage (CH_4S), water storage (H_2OS), compressed hydrogen storage (H_2St) and CO_2 storage (CO_2S). Each of these technologies comprises two sizing variables, the stock capacity and the flow capacity, and three operational variables, the inventory level, and the commodity in- and out-flows. A sixth variable is used to consider the electricity consumption needed for water storage. Equations (11 - 18) are used to model each of those technologies. The cost function in Equation 22 is minimised. Two storage technologies, pumped-storage hydroelectricity at Coo and natural gas storage at Loenhout, have fixed and pre-installed capacities. These capacities cannot be modified by the model. Note that for this model, a battery with a discharge-to-charge ratio of six was used.

Linepack (Lp). For natural gas pipeline, the linepack, the amount of gas that can be stored in the gas network, is also represented as a node. This amount is based on the actual gas network of Belgium

provided by the Belgian gas TSO. Only three operational variables, the inventory level, the commodity in- and out-flows, are considered as the flow and the stock capacities cannot be increased (that would mean an increase in the natural gas grid which is not represented in this model) and, therefore, are fixed at their existing capacities. Equations (11), (15), (19 - 20) are used to model the linepack and the cost function in Equation 22 is minimised. The linepack is not modelled for the hydrogen pipeline and CO_2 pipeline as their networks are not computed in this model.

Load shifting (LSf). The load shifting, the ability to shift a part of the demand to decrease the peak load, is modelled as a free electrical battery with pre-installed capacities that can not be increased, a limited amount of electricity that can discharged daily and obligation to refill the battery at a certain hour of the day. Similar to linepack, only three operational variables, the inventory level, the commodity in- and out-flows. Only electric demand can be shifted, the amount of electricity that can be shifted daily is based on [8]. Note that, for this study, the shifting cost is assumed to be 0. Equations (11), (15), (19 - 20) are used to model the load shifting and the cost function in Equation 22 is minimised.

Load shedding (LSd). The load shedding, the ability to shed a part of the electric demand for a very high price is modelled as a battery that can only discharge electricity and is refilled at the beginning of the day from an external source. The load shedding is modelled using five different nodes that differ in the number of hours a day their respective share of the load can be shed at their full capacity (1 hour, 2 hours, 4 hours, 8 hours and 24 hours). The amount of electricity that can be shed daily and the cost related to this shedding are based on [8]. Two variables are used, the flow capacity which is equivalent to the maximum share of the load that can be shed in one hour, and the electricity outflow. In order to keep the problem linear, the total amount of electricity that can be shed during a day by a specific load shedding node is computed by multiplying the total flow capacity by the number of hours this node allows the load to be shed. Only electric demand can be shed and contrary to its shifting, it comes with a cost (the shorter the amount of hours available a day a node of load shedding, the more expensive its use). Equation (21) is used to model the load shedding and the cost function in Equation 22 is minimised.

. Technical and economic parameters of all flexibility nodes are presented in Tables 10 - 13 in the Appendix. Economical parameters for all flexibility nodes are in 13. Table 10 and 11 gather the technical parameters for the storage while Table 12 is for linepack, load shifting and load shedding. Those parameters are based either on prediction for the year 2050 from [35] or from [8], [11] or [12].

4.2.3. Import and export nodes

Natural gas imports. The import of natural gas is considered only by pipelines in the model. The capacities of the import nodes are limited by the current existing capacities [36]. Depending on the importing country, some nodes of imports are included in the Coastal cluster (Norway (NGNO), United-Kingdom (NGUK) and France (NGFR)) while others are included in the Inland cluster (Germany (NGDE)). Only one variable is used, the quantity of natural gas imported. This variable is constrained by Equation (23) and the cost function is given by Equation (24). Note that the costs vary over time. Times series computed and provided by the Belgian natural gas TSO for the year 2015 were normalised and then

scaled to have an estimated mean value of 50€/MWh. To this cost, a tariff, reflecting the cost of using the connecting pipeline, has been added and varies from one country to another based on [37].

Synthetic methane imports (SMI). In this paper, the import of synthetic methane is possible by LNG tanker. The capacity of this node is limited by the current capacity and the regasification facilities of the port of Zeebrugge (i.e. the port of Zeebrugge is assumed to be exclusively used for the import of synthetic methane). As synthetic methane is produced remotely from CO_2 captured from the atmosphere based on the model in [12], burning it should not contribute to an increase of CO_2 in the atmosphere. To consider this specificity, the quantity of synthetic methane imported is associated with a quantity of CO_2 captured to compensate for the CO_2 released when the synthetic methane is burned. A cost of 164.8 €/MWh LHV was assumed for the import cost based on [12]. Two variables are used for this node: the amount of synthetic methane imported and the amount of CO_2 captured to produce this methane. Those variables are constrained by Equations(23) and (1). The total cost to minimise is given by the cost function (24).

Hydrogen import (H_2NL). For the import of hydrogen, it is assumed that the pipeline of natural gas connecting the Netherlands with Belgium is repurposed to be able to import hydrogen. According to recent studies [38], a repurposed pipeline of gas can transport a capacity of hydrogen in GW reaching up to 80% of its initial capacity in natural gas. Only green hydrogen is assumed to be imported. An import cost of 75 €/MWh, equivalent to approximately 2.25 €/kg of hydrogen, was considered. This aligns with the projections outlined in [39], estimating hydrogen costs to be between 1.5 to 2.5 €/kg by the year 2040. One variable is used: the amount of hydrogen imported. This variable is constrained by Equation (23). The cost function is given by Equation (24).

Electricity import. Each neighbouring country is modelled as an electricity import node. Denmark, United Kingdom, Netherlands, France, Germany, and Luxembourg are modelled. The import capacity is limited only to renewable and other emission-free capacities of these countries, and only a part of them can be imported. Those emission-free capacities are based on the capacities from [1] for the Distributed Energy scenario. Namely, 1 % of the renewable production and 30 % of the nuclear production of each neighbouring country can be imported at each time step. These two numbers are chosen arbitrarily. In practice, this forms a time series which is actually the parameter $\underline{\kappa}_t^n$ from Equation (23).

Moreover, the import capacity at any time step is also capped at the capacity of the interconnect between the country and Belgium; this parameter is called $\underline{\kappa}^{n,HV}$. Additionally, the sum of the individual amount of energy imported $q^n_{\text{elec},t}$ is capped to 1 % times the total amount of renewable and nuclear energy produced by the country over the time horizon.

The cost of energy is considered constant and is computed as the average cost of the renewable technologies in the neighbouring country and of its nuclear reactors; the cost also comprises half the price of the HV lines, the other half is assumed to be paid by the neighbour. This cost is calculated based on consistent economic assumptions applied to the conversion technologies (detailed costs provided in Table 9 in the Appendix). It incorporates a CAPEX of 1.5 M€/GW/km, with an FOM cost equivalent to 1.5% of the CAPEX for high-voltage lines. Data used to compute this cost, as well as the cost itself, is presented for each country in Table 15 in the Appendix.

Carbon dioxide export (CO_2E). CO_2 captured by DAC and PCCC is assumed be exported using a CO_2 export node. The capacity of the node is fixed at 3.5 kt/h (about 30 Mt/year) based on the same hypotheses presented in [11]. This node uses one variable: the amount of CO_2 exported. This variable is constraint by Equation (23) and the cost function is given by Equation (24).

. Technical and economic parameters for all import and export nodes are presented in Table 14 in the Appendix.

4.2.4. Transmission nodes

Transmission nodes comprise HVAC and HVDC lines, gas pipelines and hydrogen pipelines carrying energy between the three Belgium's clusters. As stated previously, these nodes allow the flow to be bi-directional using four variables, the inflow and the outflow of the commodity carried by the node in so-called *forward* and *reverse* directions. For this model, flows in the forward direction are flows going from West to East in Figure 3 while flows going in the reverse direction are going from East to West. Equations (25 - 28) are used to model each of those technologies and the cost function (29) is minimised. Technical and economic parameters of all transmission nodes are presented in Tables 16 and 17 in the Appendix. The expenses related to HVAC lines are derived from recent projects implemented by the electricity Transmission System Operator (TSO) to enhance capacities between the Offshore area and Belgium Inland. These costs factor in the expenses for cables, their corresponding substations, the offshore platform [40], and associated installations. Similarly, the costs associated with HVDC lines are drawn from [41], encompassing expenses for the offshore platform, VSC (Voltage Source Converter) converters, cables, and their respective installations.

4.2.5. Demand nodes

Demands for electricity, natural gas/methane and hydrogen are considered in this model. For each of these commodities, a demand node is designed. Each node considers four sectors: the transport, tertiary, residential and industry sectors. The final energy demands for each energy vector are given for each sector for the year 2050. Their annual values are based on the Joint Scenario Report of the Ten-Year Network Development Plans 2022 (TYNDP) co-written by ENTSOG and ENTSO-E. This report introduces three scenarios built using the supply and demand data collected from both gas and electricity TSOs. For this paper, the Distributed Energy scenario was chosen as it gives data for the year 2050 and focuses on energy autonomy. The Distributed Energy Scenario was developed using a top-down approach with full-energy perspective while proposing a pathway to reach carbon neutrality by 2050 and a 2030 emission reduction target of at least 55%. Figure 2 shows the 2050 Belgian annual demands for this scenario.

These annual values are multiplied by normalised time series from Belgian electricity and gas TSO to use realistic profiles. All the time series are taken for the year 2015.

Electrical demand time series. Three time series are used for the electricity demands:

- one time series obtained from estimation made by the Belgian electricity TSO [42] including electrical loads at both transmission and distribution levels, including residential, tertiary (excluding the heating part for these two), industry, aviation and railroad consumption with an annual value of 82.33 TWh;

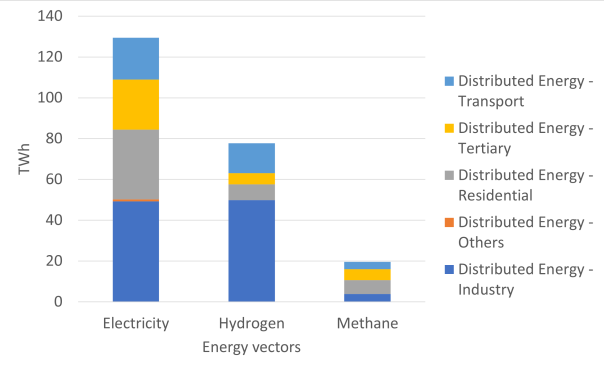

Figure 2: Belgian final energy demands for each energy vector by sector for the Distributed Energy scenario in 2050 given by the joint TYNDP of ENTSO-E and ENTSOG.

- one time series obtained from the Belgian gas TSO (Fluxys) for the heating of residential and tertiary sectors with an annual value of 30.58 TWh;
- one synthetic daily profile for electrical-based transportation, assuming a flat daily week-day and week-end travel distances, with a consumption two and a half-times higher for a week-day than for a day in the weekend with an annual value of 16.51 TWh.

Natural gas demand time series. Four time series are used for the natural gas demands:

- one time series from the electronic data platform of the Belgian gas system operator (Fluxys - Belgian's gas TSO) for the industry sector with an annual value of 3.82 TWh;
- another time series from Fluxys for the heating of residential and tertiary sectors with an annual value of 12.22 TWh;
- one time series from confidential data measured by the natural gas TSO at CNG refuelling station for road transport with an annual value of 1.1 TWh;
- a flat profile for the demand related to the shipping sector with an annual value of 2.45 TWh.

Hydrogen demand time series. Four time series are used for the hydrogen demands :

- a flat profile is assumed for the industry sector with an annual value of 49.48 TWh;
- another time series from the Belgian gas TSO for the heating of residential and tertiary sectors with an annual value of 13.24 TWh;
- the same time-series than for the CNG demand is used for the road transport with an annual value of 3.48 TWh;
- a flat time series for the demand is assumed to model the shipping, aviation and rail sectors combined with an annual value of 11.12 TWh.

The costs of energy not served for electricity, hydrogen and natural gas are set to 3000 €/MWh, 500 €/MWh and 500 €/MWh respectively based on values reported for private end users. Equations (31 - 32) are used to model the electrical demand node and Equation (30) is used to model the hydrogen and natural gas demand nodes. For all demand nodes, the cost function (33) is minimised.

4.3. Clusters

The overall architecture of the clusters is shown in Figure 3. The three main clusters (Offshore - OFF, Coastal - COA, and Inland - INL) are displayed, along with the three main commodities (electricity, gas and hydrogen). The neighbouring countries (that are modelled as import nodes) are also displayed. Each coloured square represents an interconnect (hyperedge) which ensures that there is no loss or creation of energy, i.e. that the flows are conserved. The Inland cluster can emit CO_2 and capture it, while the Coastal one can only capture it (there is no CO_2 emitting technologies modelled in this cluster). Inland can also export captured CO_2 to other countries. To guarantee carbon neutrality, the model includes a constraint that ensures the net balance of CO_2—the difference between the total amount of CO_2 emitted into the atmosphere and the total amount of CO_2 captured from the atmosphere—is zero or negative.

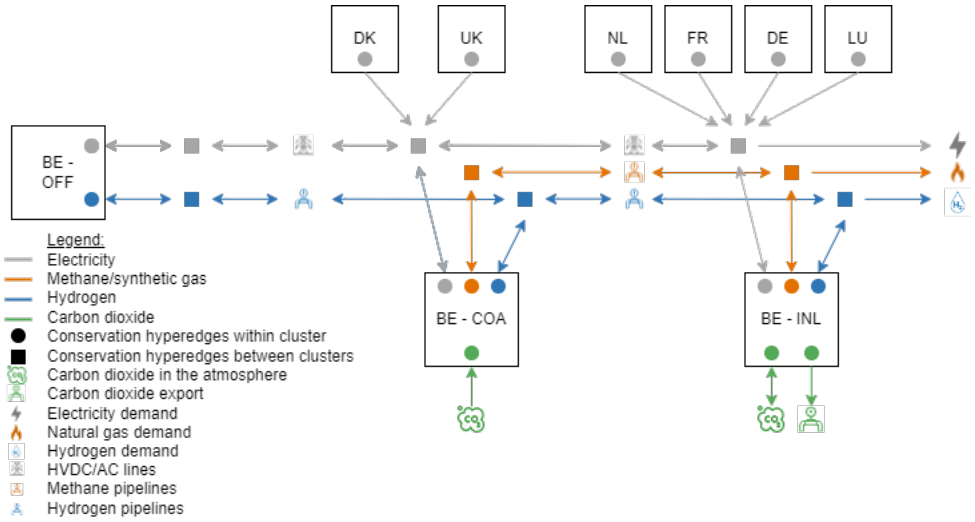

Figure 3: Simplified representation of the model with the different clusters, interconnection, flows between clusters and the different hyperedges.

In the context of the electrical interconnection linking the Belgium Inland cluster with neighbouring countries and the demand, a constraint has been established to restrict the overall flow. This constraint serves to represent the capacity of the electrical grid and has been fixed at 23 GW, determined by the peak demand in the distributed energy scenario outlined in the TYNDP. Notably, this determination does not consider the demand of the transport sector, which, in the scope of this paper, is endogenously managed.

The Belgium Offshore cluster. A schema of the Offshore cluster is shown in Figure 4. It considers two energy vectors, electricity and hydrogen, and one additional commodity, water. There are four conversion nodes (WOFF, FC, EP, DES), and three flexibility nodes (ES, H_2OS, H_2St).

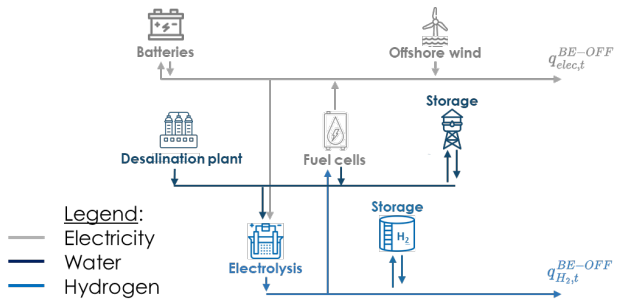

Figure 4: Schematic representation of the Belgian Offshore cluster.

Belgium Coastal cluster. The Belgium coastal cluster considers three energy vectors, electricity, hydrogen and natural gas/methane, and one additional commodity, carbon dioxide. Water flows are not considered in this cluster as the water consumed by electrolysers is assumed coming from the Belgian water network for a negligible cost. It includes 10 nodes: four conversion nodes (FC, EP, MT, DAC), two flexibility nodes (ES, H_2St), and four import nodes (NGNO, NGUK, NGFR and SMI). A schematic representation of the Belgian Coastal cluster is given in Figure 5.

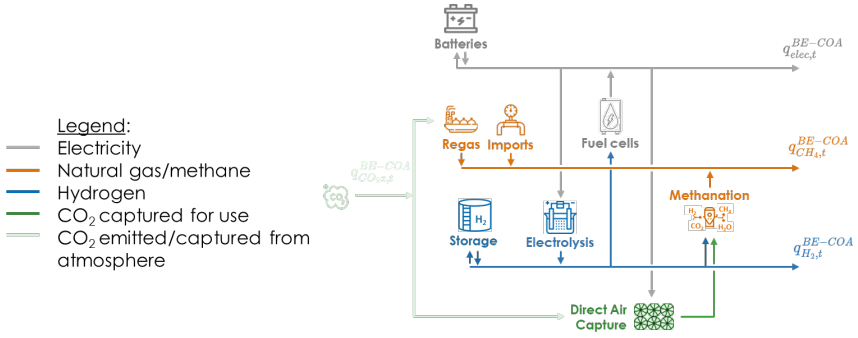

Figure 5: Schematic representation of the Belgian Coastal cluster.

Belgium Inland cluster. The Belgium inland cluster considers three energy vectors, electricity, hydrogen and natural gas/methane, and one additional commodity, the carbon dioxide. Water flows are not modelled for the same reason than in the coastal cluster. It includes 28 nodes: 13 conversion nodes (PV, WON, EP, FC, DAC, MT, BMT, CCGT, OCGT, SMR, 3 PCCCs), 12 flexibility nodes (ES, PH, CH_4S, H_2St, CO_2S, Lp, LSf and 5 LSds), two import nodes (NGDE, H2NL) and one export node (CO_2E). A schematic representation of the Belgian Inland cluster is given in Figure 6.

4.4. Scenarios

Two scenarios were investigated to determine the optimal system configuration for minimising the cost of supplying the electricity, hydrogen, and natural gas demands while ensuring the carbon neutrality of the Belgium energy system. Each scenario examined the following three technologies: offshore and onshore wind turbines and solar photovoltaic (PV) panels. However, the maximum capacities allowed for these technologies vary across the scenarios.

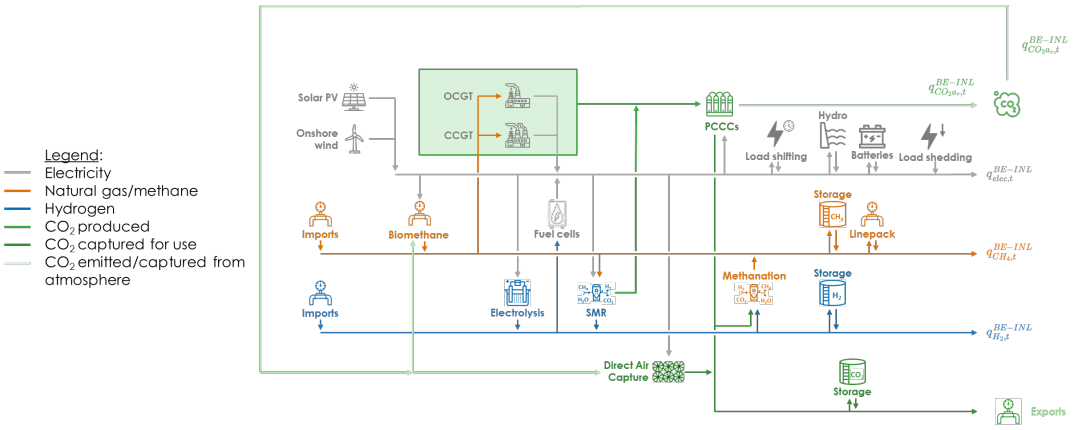

Figure 6: Schematic representation of the Belgian Inland cluster.

Scenario 1 - Base case. In the first scenario, the maximum capacities of wind turbines and solar PV panels are constrained based on the guidelines outlined in the Elia paper titled "Roadmap to Net Zero"[6]. Additionally, no nuclear power plant is installed, but there are no limitations on the quantity of direct air capture units that could be implemented.

Scenario 2 - High renewable. In the second scenario, the renewable potential is expanded based on the findings of the EnergyVille study [5], which assessed a higher renewable potential for Belgium. Similar to the first scenario, nuclear power plants are not installed, and no direct air capture units are installed.

Maximum capacities of wind turbines in the Offshore cluster, wind turbines in the Coastal cluster and the PV in the Inland cluster for each scenario in GW are displayed in Table 1. In both scenarios, it was assumed that all technologies, except for natural gas storage, pumped-hydro power plants, and existing electrical lines and natural gas pipelines within Belgium, would be completely replaced by 2050. The installed capacities of technologies in neighbouring countries were considered constant throughout the optimisation horizon. Moreover, the electrical lines and natural gas pipelines connecting Belgium to its neighboring countries were assumed to be already established and at their maximum capacities, based on future projects proposed by Elia and Fluxys.

Lastly, the pipeline connecting Belgium to the Netherlands was assumed to be repurposed for hydrogen transportation.

	$\overline{\kappa}^{WOFF}$	$\overline{\kappa}^{WON}$	$\overline{\kappa}^{PV}$
Scenario 1: Base case	8.0	9.0	50.0
Scenario 2: High renewable	9.3	20.5	103.3

Table 1: Maximum capacities of wind turbines in the Offshore cluster, wind turbines in the Coastal cluster and the PV in the Inland cluster for each scenario in GW.

5. Results & discussions

This section presents the results for the different scenarios introduced in Section 4. For the first scenario, the key results are first highlighted, then, a comprehensive analysis of the results is conducted. For the second scenario, a brief comparison for each aspect of the comprehensive analysis of the first scenario is presented.

5.1. Scenario 1 - Base case

5.1.1. Key results

Achieving carbon neutrality is feasible in the base case model, with minimal unmet demand. However, it requires a large volume of CH_4 and H_2 imports. In total, 200.5 TWh of energy are imported, constituting a substantial 58% of the total annual consumption (considering the end-user demands and the consumption of technologies). Hydrogen is predominantly imported, accounting for 97.8% of the total hydrogen supply. The remaining fraction of hydrogen, produced locally, is integrated into the coastal cluster, serving to convert electricity generated from offshore wind turbines and PV panels.

Both offshore and onshore wind energy are exploited at their maximum installable capacity with capacity factors of 22.6% and 38.2% respectively. Note that their total production is still a small share of the final electricity demand. Interestingly, carbon neutrality is reached without fully exploiting the solar PV installable capacity, due to its lower capacity factor of 11.6% and the limit on power grid capacity. Biomethane production is maximized.

Direct Air Capture (DAC) is an optimal requirement to attain carbon neutrality in this scenario. Post-Combustion Carbon Capture (PCCC) is used nearly at full capacity in the results. In total, 21.76 Mt of CO_2 is captured and all of it is exported to be sequestrated. The total system cost stands at 20.4 B€/year, equivalent to 89.87 €/MWh.

A summary of installed capacity in the optimal solution of the base case is presented in Figure 7.

5.1.2. Comprehensive analysis

Electricity production.

Figure 7 shows that wind turbines (WT) are installed at their full potential of 8 and 9 GW in the offshore and onshore areas respectively. On top of that, 28.32 GW of photovoltaic (PV) panels out of a maximum potential of 50 GW are installed. Those three renewable technologies produce 73.31 TWh annually. These energies are intermittent, as they depend on the presence of wind and sun, and thus have a known capacity factor (ratio between the energy effectively produced and the amount that could have been produced if an asset produced 100% of the time); moreover, even when the wind blows and the sun shines, curtailment may force these producers to decrease the amount of energy produced (for example in the case of low demand or due to the limit of 23 GW on the gird maximal load). In addition to the capacity factor, another metric can be used to represent this fact: the usage factor (ratio between the energy effectively produced and the energy that would have been produced without curtailment). Both metrics are reported in Table 2.

The curtailment is globally low, except for the Offshore wind turbines where just over 6% of the available energy is curtailed.

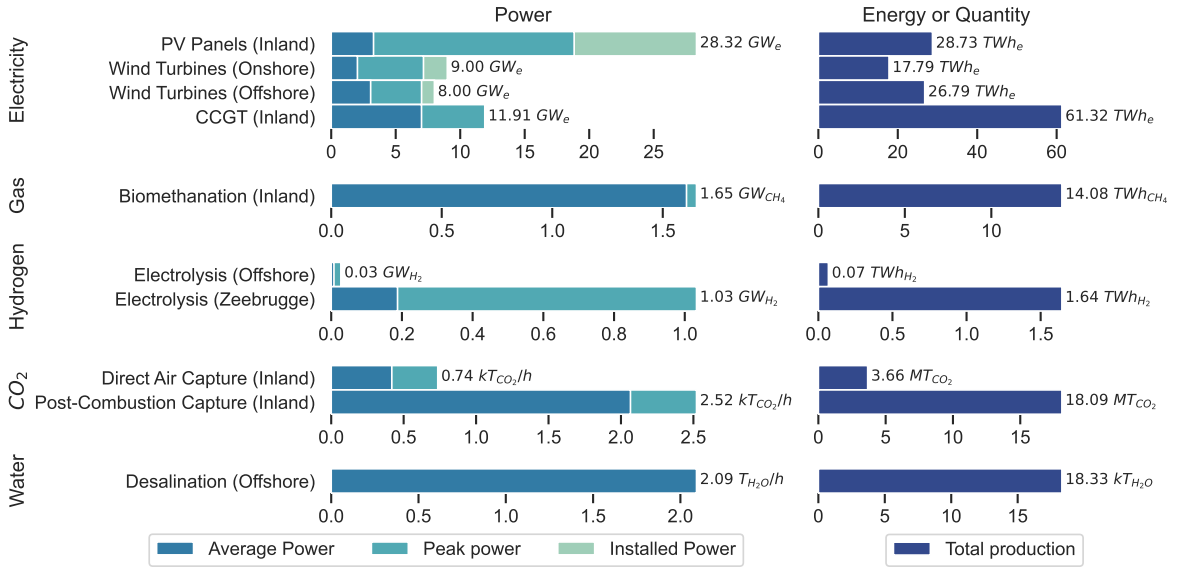

Figure 7: Installed capacities, peak power, average power and annual production of each conversion nodes.

	Total production (TWh)	Curtailment (TWh)	Capacity factor (%)	Usage factor (%)	Hours of curtailment
Photovoltaic Panels	28.73	0.50	11.58	98.30	210
Onshore Wind turbines	17.79	0.47	22.57	97.43	405
Offshore Wind Turbines	26.79	2.15	38.22	92.57	727

Table 2: Total production and curtailments of renewable technologies.

Despite the capacities installed, renewable technologies never produce at their maximum capacity for any single time step (i.e. an hour). The peak production over a time step reaches 18.83 GW for PVs, 7 GW for offshore wind turbines and 7.15 GW for onshore wind turbines.

CCGT is the only carbon emitting dispatchable technologies installed in the optimal solution (no OCGT installed). 11.91 GW are installed for a production of 61.32 TWh resulting in a capacity factor of 58.8 %. 2.52 kt/h of PCCCs are installed in order to capture a part of the CO_2 produced by CCGTs. 18.09 Mt of CO_2 are captured by PCCCs, which requires 7.46 TWh of electricity. Subtracting this consumption to the production of electricity results in a net production of 53.86 TWh of electricity annually for CCGTs.

In terms of carbon capture, 97% of the CCGT plants are fitted with a PCCC in the optimal solution. The difference can probably be considered as negligible; it is due to an optimization where, in the case when electricity is scarce, it is better to avoid starting a PCCC to capture the CO_2.

It may be counterintuitive that the installed capacity of PV is not equal to the maximal Belgian capacity; this is due to curtailment, lowering the profitability of further capacity. Note, however, that the curtailment on the wind turbines and the PV is due to the constraint we put on the electricity transport network that the power inside the network must be less than 23 GW, and the constraint that CCGTs must produce at minimum 40% of their installed capacity.

Offshore and Coastal clusters energy management.

Table 3 shows the capacities installed and the annual amount of energy flows in both directions for each transmission nodes (i.e. interconnects between the Belgian clusters). Electricity serves as the main mode of transmission, ensuring the efficient transfer of energy resources from offshore sites to onshore locations.

	K^n (GW)	Total $q^n_{i_f,t}$ (TWh)	Total $q^n_{i_r,t}$ (TWh)
HV lines OFF - COA	6.84	26.70	0.04
HV lines COA - INL	6.54	28.97	1.13
H_2 pipelines OFF - COA	0.03	0.07	0.00
H_2 pipelines COA - INL	1.06	1.71	0.00
CH_4 pipelines COA - INL	60.50	78.77	0.00

Table 3: Capacities in the forward direction, K^n_f, annual amount of the flow in the forward direction, Total $q^n_{i_f,t}$, and annual of the energy flow in the reverse direction, Total $q^n_{i_r,t}$, of each transmission nodes installed.

In contrast, the production of hydrogen offshore is negligible and its total production amounts to 1.71 TWh, particularly within the Coastal cluster. Electrolysers are preferred for hydrogen production in the Coastal cluster due to economic considerations. The utilization of electrolysers there helps reduce the cost of interconnections by installing H_2 pipeline instead of high-voltage lines.

A noteworthy aspect of the energy flow is the bidirectional movement of electricity at transmission nodes. Electricity generated in the inland cluster is converted into hydrogen within the Coastal cluster. In the overall energy balance, 2.31 TWh of electricity is required to produce 1.71 TWh of hydrogen. Both inland and offshore energy are used to produce hydrogen in the Coastal cluster: out of this total, 1.13 TWh is sourced from inland production, and 1.18 TWh is derived from offshore wind turbines.

	E^n (GWh or kt)	K^n (GW or kt/h)	Peak q^n_i (GW or kt/h)	Peak q^n_j (GW or kt/h)	# cycles
OFF Batteries	1.14				147
(Charge)		0.13		0.13	
(Discharge)		0.75	0.75		
COA Batteries	10.36				153
(Charge)		1.16		1.16	
(Discharge)		6.98	5.76		
INL Batteries	16.25				170
(Charge)		1.47		1.47	
(Discharge)		8.81	8.81		
OFF H_2O storage	1.67	5.29e-3	5.29e-3	1.72e-3	7

Table 4: Stock capacities, E^n, flow capacities, K^n, peak discharge, Peak q^n_i, peak charge, Peak q^n_j and number of cycles of each storage technologies installed in the optimal solution of the Base Case scenario.

Table 4 shows the different storage capacities. Technologies not mentioned were not used by the optimal solution of the model. For electrical batteries, the flow capacity is presented for both charge and discharge. 1.14 GWh of electrical batteries with discharge and charge flow capacities of 0.75 and 0.13 GW respectively are installed in the Offshore cluster. To deliver water to the Offshore cluster electrolysers,

2.09 t_{H_2O}/h of desalination plants coupled with 1.67 kt of water storage are installed. In the Coastal cluster, 10.36 GWh of electrical batteries with discharge and charge flow capacities of 6.98 GW and 1.16 GW, respectively, are installed. Their usage is a result of the optimisation and can be explained by three factors:

- to delay the delivery of offshore wind turbine electricity during its peak production;
- to delay the delivery of offshore wind turbine electricity when the production of electricity in the Inland cluster exceeds the consumption;
- during spring and summer, to store in coastal-located batteries a part of the electrical energy coming from inland PV panels.

These cases are illustrated in Figure 8, depicting the electricity balance within the coastal area for both a winter day and a summer day. The observed delay in electrical production from wind turbines accounts for the slightly reduced capacity of high-voltage (HV) lines (7 GW peak for offshore wind turbines but 6.84 GW of HV-lines installed), as mentioned earlier. Nevertheless, curtailment persists in the output of offshore wind turbines.

No H_2 storage, fuel cells, direct air capture or methanation plants are installed in the Offshore and Coastal clusters.

Inland cluster energy management.

In addition to renewable technologies, 16.25 GWh of batteries with a discharge capacity of 8.81 GW are also installed in the Inland cluster. 740 t/h direct air capture units and 1.69 GW of biomethanation are installed as well. The latter two technologies help to compensate for the CO_2 emitted from the combustion of gas by capturing 3.66 Mt of CO_2 for the DAC and by avoiding 2.84 Mt of CO_2 emitted in the air due to production of 14.08 TWh of biomethane. With the addition of 18.09 Mt of CO_2 captured by PCCCs, 21.75 Mt of CO_2 are captured in total. To provide a sense of magnitude, this quantity signifies nearly 50% of the total volume of CO_2 captured globally in 2022, as reported by the International Energy Agency (IEA) [43].

Figure 9 shows that the electricity consumption for the capture of CO_2 and the production of electrolysis reach their highest values between May and August. It follows that electricity produced by PVs are the main source of electricity for DAC and EPs and that DAC is used when final demand is lower.

Despite both disposing of available capacity, neither hydro-pumped storage or CH_4 storage are used. For hydro-pumped storage, it is due to the fact that its round-trip efficiency is lower than the round-trip efficiency of the electrical batteries. In order to avoid electrical losses, electrical batteries are preferred despite their investment costs being the highest. For CH_4 storage, this is caused by the import of natural gas by pipeline which follows the natural gas demand. Moreover, the difference in costs between winter and summer for the natural gas imported is not a large enough incentive for the usage of the natural gas storage.

Neither hydrogen nor synthetic methane are produced in the Inland cluster and no CO_2 storage is installed.

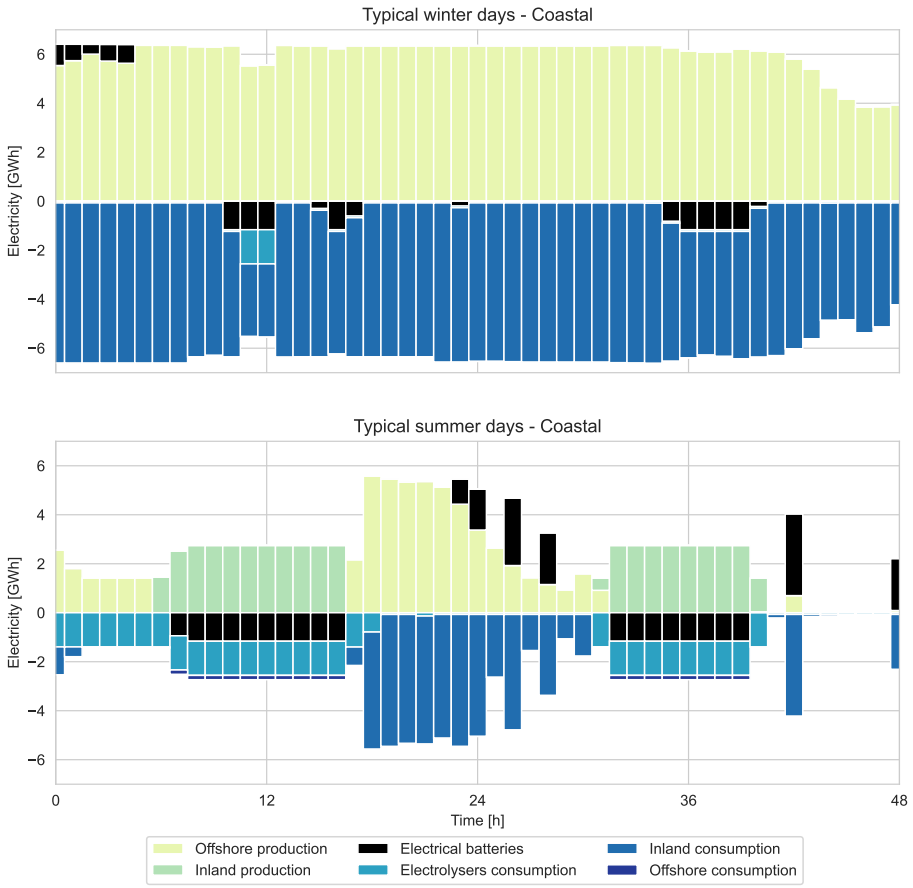

Figure 8: Electricity balance in the Coastal area for two winter-specific days on the upper and two specific summer days on the lower.

Import and Export.

Table 5 shows the amount of energy imported or exported and the peak value of the energy imported or exported for each import and export node and neighbour country cluster. In total, 16.74 TWh of electricity, 75.97 TWh of hydrogen and 107.77 TWh of natural gas are imported.

For the import of electricity, the biggest exporters are the United Kingdom, France and Germany from which 4.75, 5.53 and 3.36 TWh are imported respectively. For France and United Kingdom, it is due to the presence of nuclear power plants exporting massively during the winter. Germany has by hypothesis the most renewable technologies installed, leading to a higher amount of energy available for import. From the remaining exporter countries, Denmark, Netherlands and Germany, 0.92, 2.17 and 0.01 TWh of electricity are imported respectively. The peak power of imported electricity reaches the existing interconnect capacity only for United Kingdom and Germany. For the other countries, constraint 23 limiting the hourly amount of electricity that can be imported prevents their peak power from reaching the existing interconnect capacity.

For the import of green molecules, 75.97 TWh of hydrogen are imported from the Netherlands, which

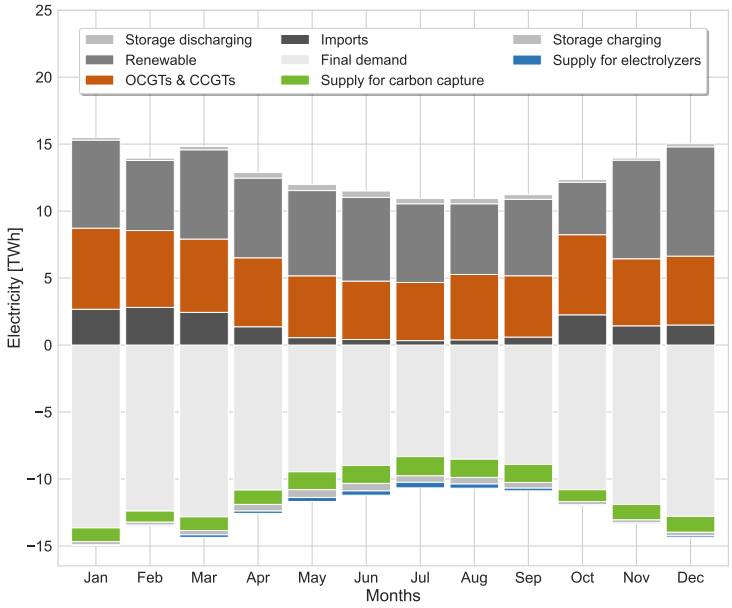

Figure 9: Electricity balance of the entire system for each month of the year.

represent 97.8 % of the annual hydrogen demand. No synthetic methane is imported by ship. It is still less expensive to import natural gas, 78.77 TWh from France and 29 TWh from Germany, capture the CO_2 emitted from their combustion and export it than import synthetic natural gas. 21.76 Mt of CO_2 is exported annually out of the 30 Mt possible.

Demand side management and energy not served.

Table 6 shows the capacities, the annual amount load reduction, the number of hours each flexibility node (related to demand side management) reduces the load, or the energy is not served. The predominant method of flexibility utilization involves electrical load shifting, which annually displaces 56.25 GWh out of the available 547.5 GWh. Furthermore, load shedding nodes contribute to shedding 31.34 GWh of load. Even with these load-shifting and shedding measures in place, there remains an unmet electricity demand of 2.31 GWh annually, constituting a mere 0.002% of the total annual end-user electricity demand.

As expected, the load tends shift from peak hours of consumption occurring at the beginning and the end of the day to peak hours of production, especially of solar production. Load shedding occurs especially during "dunkelflaute", i.e., during period of time when the production of electricity from PV panels and wind turbines is very low or non existent while the consumption is high.

Costs.

Figure 10 shows the annual costs relative to each node and neighbour country clusters. For conversion, flexibility and transmission nodes, these annual costs consider the investment, operational and maintenance costs. For conversion nodes requiring a specific fuel (biomass for biomethanation plants for example), fuel costs are also included in the annual costs. For conversion technologies emitting or capturing CO_2, tax costs relative to CO_2 emitted or subsidies relative to CO_2 captured are comprised as

	Preinstalled capacity κ^n (GW or kt/h)	Total energy q_i^n (TWh or Mt)	Peak power q_i^n (GW or kt/h)
Elec Denmark	2.00	0.92	0.38
Elec United Kingdom	2.40	4.75	2.40
Elec Luxembourg	1.00	0.01	0.01
Elec France	8.30	5.53	5.43
Elec Netherlands	5.40	2.17	1.05
Elec Germany	1.00	3.36	1.00
INL H_2 Netherlands	25.65	75.97	12.28
COA NG Norway	18.35	0.00	0.00
COA NG United Kingdom	24.50	0.00	0.00
COA NG France	9.37	78.77	9.37
COA SG North Africa	26.81	0.00	0.00
INL NG Germany	15.06	29.00	15.06
INL CO_2	3.50	21.76	3.26

Table 5: Flow capacities, κ^n, annual energy imported or exported, Total q_i^n and peak energy imported or exported of each import and export nodes and neighbor country clusters.

	K^n (GW)	Total q_i^n (GWh)	# hours
Load shifting	1.500	56.25	142
Load shedding 1h	0.128	0.256	2
Load shedding 2h	0.446	1.784	4
Load shedding 4h	0.534	4.272	9
Load shedding 8h	0.383	7.403	21
Load shedding 24h	0.300	17.621	59
Energy not served electricity	3.156	2.311	9
Energy not served hydrogen	0.000	0.000	0
Energy not served natural gas	0.000	0.000	0

Table 6: Flow capacities or max energy not served, K^n, annual load reduction, Total q_i^n and number of hours of each flexibility nodes reduce the load or the energy is not served

well. For import and export nodes and neighbour country clusters, the annual costs are proportional to the annual amount of the commodity either imported or exported from or to the nodes and clusters.

This figure shows that the highest costs are from the import of molecules. It is worth mentioning that this is mainly due to the large quantity imported. Indeed, almost all hydrogen and natural gas demands is supplied by importing from the Netherlands and from both France and Germany, respectively. 58% of the primary energy demand is met from imports. The next highest costs are related to technologies producing electricity: PV, CCGT and WT. Moreover, the cost of capturing CO_2 from CCGT is nearly the same as the cost of CCGT itself. The last significant cost is imputed to biomethane production. The remaining costs are less impactful than the ones aforementioned. Finally, the total cost of the system, i.e., the sum of all costs given in the figure, is 20.4 B€/y, resultant in an average cost of 89.87 €/MWh of final energy demand.

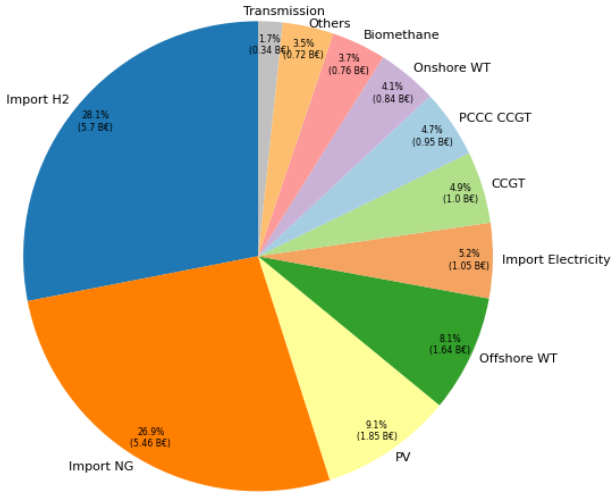

Figure 10: of Costs of each node and neighbouring clusters

5.2. Scenario 2 - High renewable

5.2.1. Comparison

The results from simulation of scenario 2 are shown in Figure 11. Other tables and figures related to results of this scenario are found in the Appendix.

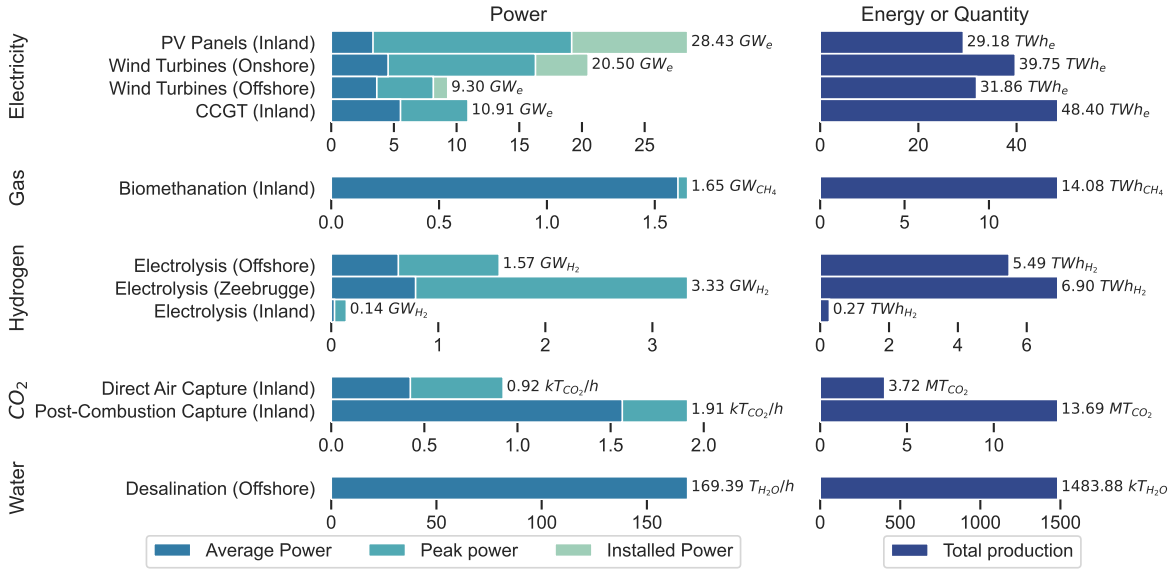

Figure 11: Installed capacities, peak power, average power and annual production of each conversion nodes.

Electricity production.

Wind Turbine have the maximal capacity and are bigger than in the first scenario: 20.5 GW for the Onshore cluster and 9.3 GW for the Offshore cluster compared to 9 GW and 8 GW respectively. Solar PV

remains similar at 28.48 GW. Moreover, since the production of green electricity surpasses the Base Case (100.79 vs 73.31 TWh for Base Case), there is a decrease in CCGT production, resulting in a reduced need for capturing CO2.

Offshore and Coastal clusters energy management.

In the High Renewable scenario, offshore hydrogen production becomes significant, reaching 5.49 TWh, a stark contrast to its negligible presence in the Base case as it was limited by the renewable energy potential. This shift signifies a notable rise in energy from offshore sources directly converting into hydrogen. Consequently, it requires deploying 1.57 GW of electrolysers and 169.39 $t_{H_2O/h}$ of offshore desalination.

Within the Zeebrugge Coastal cluster, the electrolyser capacity has surged from the initial 1.03 GW in the Base Case to 3.33 GW, leading to a fourfold increase in hydrogen production. This boost stems from the amplified generation of green electricity in this specific scenario.

The capacities of HVAC lines and hydrogen pipelines are also affected, as shown in Table 19 in the Appendix. With increased H_2 production, pipelines require adjustments to accommodate increased transportation, while HVAC lines can be smaller due to decreased electricity transportation.

Import and Export.

The import of hydrogen decreases in this scenario as more hydrogen is produced domestically. Additionally, there is a reduction in the import volume of natural gas due to its decreased use in electricity generation (as there is more electrical energy produced from wind turbines). In total, 151.27 TWh of energy are imported, constituting a substantial 51.3% of the total annual consumption. However, the volume of electricity imported remains relatively constant.

Regarding exports, the diminished production of CO_2 and subsequent lower capture levels lead to a decrease in the exported quantity (from 21.76 Mt/year for the Base case scenario to 17.41 Mt/year for the high renewable scenario). Detailed numerical values can be located in Table 21 within the appendix.

Demand-side management and energy not served.

Load shifting and load shedding in this scenario are in the same order of magnitude as the Base Case scenario. They are still a small fraction of the year's demand and can be considered as insignificant as the first scenario (about 0.06 %). The precise results can be seen in Table 22 in the Appendix.

Costs.

The total annual cost of the system is 19.77 B€/y compared to 20.39 B€/y for the Base Case. The detail costs have the same trends as Scenario 1 and are shown in the appendix. This results in an energy cost of 85.44 €/MWh compared to 89.84 €/MWh. This is roughly a 5% saving by year compared to the Base Case scenario.

6. Sensitivity analysis

This analysis is conducted to study the factors influencing the offshore production of H_2.

The production and transportation of hydrogen are central points in the decision to use electrons or hydrogen for offshore energy transportation. Indeed, their costs can be a deterrent and thus lead to the use of electrons. It is therefore important to study the behaviour of factors that influence these costs. In this sensitivity analysis, two factors are studied:

- the impact of the H_2 import price is assessed, which can help identify a threshold beyond which importation is no longer profitable compared to offshore production.
- the distance between offshore and coastal clusters is examined to determine if there exists a distance between these two for which hydrogen pipelines can surpass electrical lines, that are generally more profitable.

This analysis was conducted on both scenarios but as the conclusions are qualitatively the same, for conciseness, only results for the Base Case scenario are presented.

6.1. Sensitivity analysis on the price of H_2 imports

This section delves into analysing the model's behaviour in response to fluctuations in the price of H_2. In previous simulations, this price was fixed at 75 €/MWh, equivalent to 2.5 €/kg. In this sensitivity analysis, we explore a range from 75 to 300 €/MWh. The primary goal is to understand how the model addresses the hydrogen demand and assess its impact on CO_2 emissions and electricity production.

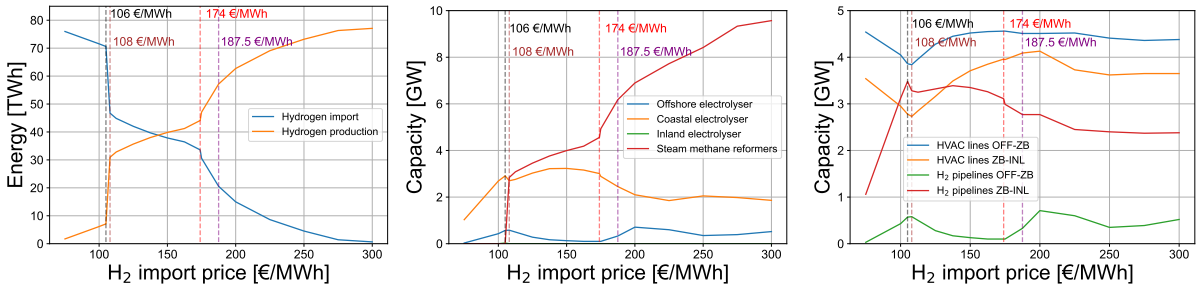

(a) Evolution of the production of H_2 from hydrogen production technologies and the import of H_2.

(b) Evolution of capacities installed of hydrogen production technologies.

(c) Evolution of capacities installed of transmission technologies.

Figure 12: Impact of the cost of H_2 import on the production and the import of H_2.

Figure 12a shows that the amount of imported hydrogen decreases as the price of importing H_2 increases, dwindling to a negligible amount at 300 €/MWh.

Regarding the offshore hub, raising the cost of imported H_2 initially boosts the production of electrolysers there, as depicted in Figure 12b. At 106 €/MWh (3.53 €/kg), electrolysis plants in the Offshore area hit their peak capacity at 620 MW, generating 2.1 TWh. Consequently, the required capacity for new electricity transmission lines decreases from 4.54 GW to 3.8 GW.

However, at this price, the majority of hydrogen is still produced in Zeebrugge, with a capacity of 2.86 GW and a production of 7.3 TWh (compared to 1.03 GW and a production of 1.6 TWh at 75 €/MWh). Additionally, most of the consumed hydrogen comes from imports, with 70.4 TWh imported and only 7.3 TWh produced.

Beyond 106 €/MWh, steam methane reformers become profitable for producing H_2, but with added costs linked to treating its CO_2 emissions (PCCC units, DAC needed for capturing remaining CO_2, and CO_2 export). The reason why hydrogen isn't entirely produced by SMR is due to the limit on CO_2 exports, as illustrated in Fig 13b.

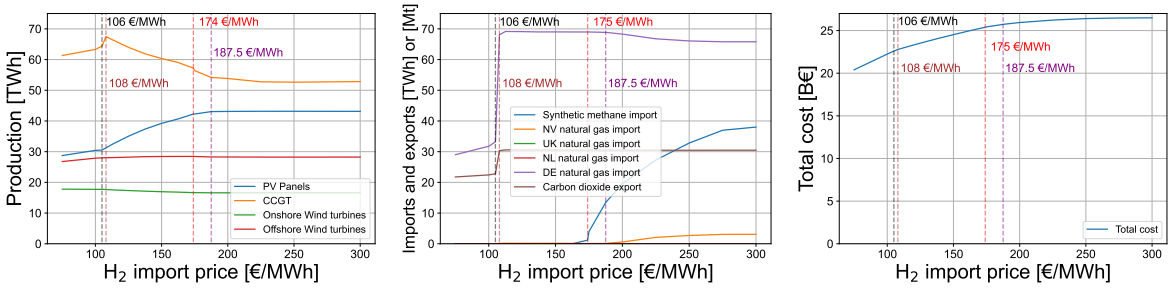

(a) Evolution of production of electricity from PV and CCGT.

(b) Evolution of the import of natural gas and synthetic methane.

(c) Total cost of the system.

Figure 13: Impact of the cost of H_2 imports on the result of the Base Case scenario.

When the electricity price reaches 108 €/MWh, the CO_2 export limit is reached, resulting in a balance between the production of CCGT and Steam Methane Reforming (SMR). Between 108 €/MWh and 187.5 €/MWh, an increase in SMR production causes a decrease in electricity generated from CCGT. To compensate for the shortage, PVs generate more electricity, while electrolysers production slightly decreases. Beyond 174 €/MWh, it becomes profitable to import synthetic methane, enabling SMR to produce hydrogen without capturing all emitted CO_2.

At 187.5 €/MWh, PVs reach their maximum capacity. To offset the reduced CCGT production, less hydrogen is produced from green electricity. Imports of synthetic methane further increase for SMR hydrogen production. Around 300 €/MWh, only a negligible amount of hydrogen is imported, with the majority being produced by SMR.

6.2. Sensitivity analysis on the distance between Offshore cluster and Coastal clusters

In this section, the impact of the distance between the Offshore and Coastal clusters is studied. In previous simulations, the length was set at 40 km for HVAC lines. In the following simulations, HVAC lines are used for distance between 40 and 80 km. Above 80 km HVDC lines are used. The range selected for the length varies from 40 km to 1000 km.

As the distance increases, the difference in cost between HV lines and hydrogen pipelines becomes more pronounced. Between 40 km and 500 km, extending the distance between the Offshore and Coastal clusters favours offshore hydrogen production (from 0.11 TWh at 50 km to 3.2 TWh at 500 km) as illustrated in Fig. 14. Hydrogen production in Zeebrugge decreases, resulting in an overall rise in the total amount of H_2 produced (from 1.7 TWh at 40 km to 3.3 TWh at 500 km). Despite the extended

distances, most of the energy generated offshore is transmitted as electricity (23.1 out of 28.8 TWh at 500 km), while a substantial amount of the hydrogen is still sourced from imports (74.4 TWh out of 77.7 TWh consumed at 500 km).

Beyond 500 km, offshore wind turbine production starts to decline as it becomes less financially viable due to the expenses associated with transmission lines. At this point, there is a preference for electricity production from CCGT (as illustrated in Fig. 15) and importing hydrogen.

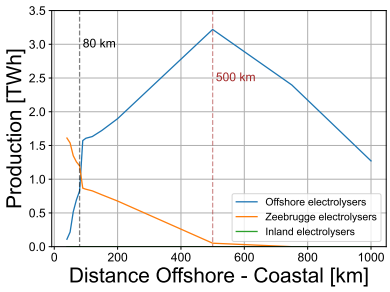

Figure 14: Evolution of the production of H_2 from electrolysis plants.

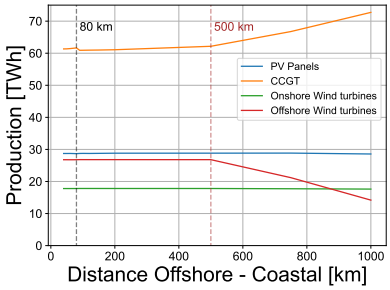

Figure 15: Evolution of the production of electricity.

6.3. Conclusion

The rise in both the import price of H_2 and the distance between the Offshore and Coastal clusters impacts H_2 production. As anticipated, both factors result in increased domestic production. However, the majority of energy generated by offshore wind turbines is still transmitted as electricity. When the import price rises, most H_2 is produced by SMR. Regarding the distance increase, a maximum of 3.3 TWh of hydrogen is annually produced from offshore electrolysis out of the 26.8 TWh of electricity generated by offshore wind turbines. We highlight that Belgium's renewable electricity potential limitation restricts the availability of green electricity for hydrogen production.

7. Limitations

Many hypotheses are scattered throughout the text. For the sake of clarity, we summarize and discuss the main ones here.

In Section 3, we introduce multiple assumptions, which each pose some limitations on the results. The concept of central planning and operation assumes a perfectly competitive market, disregarding the reality of multiple influential actors and factors in the market. Similarly, the perfect foresight and knowledge assumption fail to account for uncertainties in demand, operations, and weather conditions. Moreover, investment and operational decisions rely on a database of cost predictions established in 2021, neglecting recent increases in material costs, and, of course, future unpredictable modification to these costs in the next years up to 2050. Additionally, assumptions about technologies and processes models overlook startup time, artificially increasing the response time of some technologies. CCGTs, which form a large part of any optimal solution in the model, are modelled such that they need to be running at least at 40% capacity, rather than allowing them to shut down. The above assumptions are employed to maintain the model's size to a manageable one and ensure efficient computation, albeit at the expense of overlooking certain complexities.

A limit was set on the total flow of electricity to avoid unrealistic peaks in the electricity network. A value of 23 GW was decided based on the peak of the electricity demand used in the model. Allowing the possibility of increasing this limit with a cost related to an added capacity could change the results especially in the number of PVs installed. Another significant limit is on nuclear power generation, which Belgium has currently 4 GW of. Belgium's stance on nuclear power excludes it from the country's future electricity production plans. However, plans can change and nuclear energy could still play a significant role in Belgium's hydrogen production—a possibility worth exploring in future research.

Another assumption is that imported electricity comes from decarbonized sources, imposing a cap on the quantity of electricity available for import at each time step. While the model aims to promote local production, other assumptions within it could influence the outcomes.

Gas imports are solely restricted by pipeline capacity, and Belgium, serving as a transit nation, mostly imports natural gas that is subsequently exported to other countries. This limitation in practice affects the volume of natural gas and influences its pricing. A comprehensive investigation would be necessary, although it falls beyond the scope of this paper [44].

The energy demand relies on TYNDP predictions [1], but it is important to note that demand and supply are related. A rise in costs typically leads to a drop in consumption, as we have seen during the last year. While estimating the elasticity of the supply-demand curve is beyond this paper's scope, for simplicity, demands are input of the problem as time-series.

Another important assumption was the possibility to export CO_2 and to store it abroad. This assumption allows for the use of carbon capture technologies and limits the quantity of carbon that can be captured. It is a significant assumption since it allows the model to use carbon-emitting technologies in the energy mix while still being able to reach carbon neutrality.

The model was simulated for only one year. While running it for multiple years (or for slight modifications of the data related to the same year) could produce more robust results, the focus was not

primarily on achieving pinpoint accuracy regarding installed capacity. Instead, the goal was to assess the impact of specific hypotheses (namely the costs linked to H_2 imports, and the distance between the offshore cluster and the coastal one, see Section 5) and to gain a deeper understanding of the system's dynamics (Section 6).

8. Conclusion and future works

In this work, we modelled a hypothetical energy system for 2050, modelling various commodities, e.g., gas, electricity and hydrogen, and technologies, e.g., wind turbines, solar PV panels. Particular attention was paid to both the carbon neutrality and a geographical separation. This separation was conducted between three *clusters* : the Inland, the Offshore and the Coastal. The former one considers the consumption and production happening within the boundary of the country, the second in the North Sea and the latter at the coast. These clusters are linked by HV lines and pipelines.

By using the TYNDP prediction for demand in 2050 from ENTSO-E and ENTSOG, we compute the optimal sizing for energy production in 2050, in order to estimate which technologies should be included, notably offshore and to assess the need to convert offshore energy into hydrogen in order to be transmitted to coastal rather than to use HV lines.

At our default assumptions of 2.5€/kg for the price of H_2 imports and a distance of 40 kms between the offshore area and the coast of Belgium, we obtain that the optimal sizing for offshore wind turbines is to install 8 GW producing 26.79 TWh; most of the energy transits via high voltage lines while a negligible amount is converted to hydrogen and transits via pipelines to the coast.

In order to test the sensibility of these results to our assumption, we tried three variations of the model.

First, we increased the maximum potential for renewable production in the model (both inland, for PVs and wind turbines, and for offshore wind turbines). This led to a significant increase in the offshore H_2 production, increasing from a negligible amount to nearly 5.5 TWh.

Second, we considered what happens if the price of H_2 import substantially increases. As the price increases, the amount of production of offshore hydrogen tends to increase but its value greatly varies depending on the cost of other technologies, such as steam methane reforming.

Last, we analysed the impact of the distance between the coast and the offshore clusters. Any increase of the distance, up to 80 km (where the electricity transmission technology switches to HVDC in the model), leads to a substantial increase of the H_2 production offshore. Above 80km, the increase is slower but still substantial, and peaks at 500 km at 3 TWh of H_2. Going above 500km makes the electricity and hydrogen costs too high to be profitable compared to inland production, and the production subsequently decreases.

Overall, the analyses tend to show that depending on several important factors (distance to the coast, price of hydrogen imports, solar and wind capacity), offshore H_2 production, and in general power-to-H_2, can contribute effectively to a decarbonised energy system at a competitive cost.

This work can be extended through several interesting paths. As the potential of renewable energy seems to be the most important factor for the production of offshore hydrogen, extending this model by

adding more countries with more renewable resources could lead to interesting results. This would offer greater precision while handling the exchanges between countries for all commodities as well.

Furthermore, the granularity of the Belgian model itself can be more precise. This can be achieved by modelling both transmission and distribution networks for hydrogen, natural gas and electricity. This would allow Belgian authorities to have a precise insight of the future of the different networks. Other improvements to the model could include making energy demand endogenous for heating and transport, adding missing energy vectors such as biomass, oil, and coal, and studying pathways from the present to the solution for 2050.

Finally, a focus on the potential of the North Sea as an individual cluster can also be considered. As it is a key spot for renewable production (wind) and it can be used an exchange spot between countries.

Acknowledgements

The authors gratefully acknowledge the support of the Federal Government of Belgium through its Energy Transition Fund and the INTEGRATION project.

Author contributions:

Jocelyn Mbenoun: Conceptualization, Methodology, Validation, Formal Analysis, Investigation, Writing - Original Draft, Visualization. **Amina Benzerga:** Validation, Writing - Original Draft, Writing - Review & Editing, Visualization. **Bardhyl Miftari:** Conceptualization, Methodology, Validation, Writing - Original Draft, Writing - Review & Editing, Visualization. **Ghislain Detienne:** Conceptualization, Writing - Review & Editing. **Thierry Deschuyteneer:** Conceptualization, Writing - Review & Editing. **Juan Vazquez:** Conceptualization, Writing - Review & Editing. **Guillaume Derval:** Methodology, Formal Analysis, Writing - Review & Editing, Supervision. **Damien Ernst:** Conceptualization, Methodology, Writing - Review & Editing, Supervision.

Declaration of competing interest

The authors declare no conflicting financial or personal interests.

Declaration of Generative AI and AI-assisted technologies in the writing process

During the preparation of this work the authors used chat.gpt for minor word checks and rephrasing. After using this tool, the authors reviewed and edited the content as needed and take full responsibility for the content of the publication.

References

[1] TYNDP 2022 - scenario export (2022).

[2] P. Capros, A. De Vita, N. Tasios, P. Siskos, M. Kannavou, A. Petropoulos, S. Evangelopoulou, M. Zampara, D. Papadopoulos, C. Nakos, et al., Eu reference scenario 2016-energy, transport and ghg emissions trends to 2050. (2016).

[3] G. Limpens, H. Jeanmart, F. Maréchal, Belgian energy transition: what are the options?, Energies 13 (1) (2020) 261.

[4] D. Devogelaer, D. Gusbin, J. Duerinck, W. Nijs, Y. Marenne, M. Orsini, M. Pairon, Towards 100% renewable energy in belgium by 2050 (2012).

[5] F. M.-H. Wim Clymans, Karolien Vermeiren, How much renewable energy can be generated within the belgian borders? (dynamic energy atlas) (2021).
URL `https://www.energyville.be/en/press/how-much-renewable-electricity-can-be-generated-within-belgian-borders-dynamic-energy-atlas`

[6] Roadmap to net zero elia group's vision on building a climate-neutral european energy system by 2050 (2021).

[7] The potential to reduce co2 emissions by expanding end-use applications of electricity, 1018871 (2009).

[8] Adequacy and flexibility study for belgium 2022 - 2032 (2021).

[9] IEA, Offshore wind outlook 2019, Technical Report (2019).

[10] A. Wang, J. Jens, D. Mavins, M. Moultak, M. Schimmel, K. van der Leun, D. Peters, M. Buseman, et al., Analysing future demand, supply, and transport of hydrogen (2021).

[11] M. Berger, D. Radu, R. Fonteneau, T. Deschuyteneer, G. Detienne, D. Ernst, The role of power-to-gas and carbon capture technologies in cross-sector decarbonisation strategies, Electric Power Systems Research 180 (2020) 106039.

[12] M. Berger, D. Radu, G. Detienne, T. Deschuyteneer, A. Richel, D. Ernst, Remote renewable hubs for carbon-neutral synthetic fuel production, Frontiers in Energy Research 9 (2021) 671279.

[13] S. M. Dawoud, X. Lin, M. I. Okba, Hybrid renewable microgrid optimization techniques: A review, Renewable and Sustainable Energy Reviews 82 (2018) 2039–2052.

[14] A. Maroufmashat, M. Fowler, S. S. Khavas, A. Elkamel, R. Roshandel, A. Hajimiragha, Mixed integer linear programing based approach for optimal planning and operation of a smart urban energy network to support the hydrogen economy, International Journal of hydrogen energy 41 (19) (2016) 7700–7716.

[15] M. S. Diéguez, A. Fattahi, J. Sijm, G. M. España, A. Faaij, Linear programing formulation of a high temporal and technological resolution integrated energy system model for the energy transition, MethodsX 9 (2022) 101732.

[16] B. Miftari, M. Berger, H. Djelassi, D. Ernst, Gboml: Graph-based optimization modeling language, Journal of Open Source Software 7 (72) (2022) 4158.

[17] R. Fourer, D. M. Gay, B. W. Kernighan, A modeling language for mathematical programming, Management Science 36 (5) (1990) 519–554.

[18] W. E. Hart, J.-P. Watson, D. L. Woodruff, Pyomo: modeling and solving mathematical programs in python, Mathematical Programming Computation 3 (2011) 219–260.

[19] T. Brown, J. Hörsch, D. Schlachtberger, Pypsa: Python for power system analysis, arXiv preprint arXiv:1707.09913 (2017).

[20] S. Pfenninger, B. Pickering, Calliope: a multi-scale energy systems modelling framework, Journal of Open Source Software 3 (29) (2018) 825.

[21] P. Mancarella, Mes (multi-energy systems): An overview of concepts and evaluation models, Energy 65 (2014) 1–17.

[22] M. Geidl, G. Andersson, Operational and structural optimization of multi-carrier energy systems, European transactions on electrical power 16 (5) (2006) 463–477.

[23] S. Collins, J. P. Deane, K. Poncelet, E. Panos, R. C. Pietzcker, E. Delarue, B. P. Ó. Gallachóir, Integrating short term variations of the power system into integrated energy system models: A methodological review, Renewable and Sustainable Energy Reviews 76 (2017) 839–856.

[24] A. Belderbos, T. Valkaert, K. Bruninx, E. Delarue, W. D'haeseleer, Facilitating renewables and power-to-gas via integrated electrical power-gas system scheduling, Applied Energy 275 (2020) 115082.

[25] The modular hub-and-spoke concept has substantial societal benefits and thus the potential to incentivise all involved stakeholders (2019).

[26] A. Singlitico, J. Østergaard, S. Chatzivasileiadis, Onshore, offshore or in-turbine electrolysis? techno-economic overview of alternative integration designs for green hydrogen production into offshore wind power hubs, Renewable and Sustainable Energy Transition 1 (2021) 100005.

[27] O. S. Ibrahim, A. Singlitico, R. Proskovics, S. McDonagh, C. Desmond, J. D. Murphy, Dedicated large-scale floating offshore wind to hydrogen: Assessing design variables in proposed typologies, Renewable and Sustainable Energy Reviews 160 (2022) 112310.

[28] A. Dadkhah, G. Van Eetvelde, L. Vandevelde, Optimal investment and flexible operation of power-to-hydrogen systems increasing wind power utilisation, in: 2022 IEEE International Conference on

Environment and Electrical Engineering and 2022 IEEE Industrial and Commercial Power Systems Europe (EEEIC/I&CPS Europe), IEEE, 2022, pp. 1–6.

[29] C. Thommessen, M. Otto, F. Nigbur, J. Roes, A. Heinzel, Techno-economic system analysis of an offshore energy hub with an outlook on electrofuel applications, Smart Energy 3 (2021) 100027.

[30] B. Miftari, M. Berger, G. Derval, Q. Louveaux, D. Ernst, Gboml: a structure-exploiting optimization modelling language in python, Optimization Methods and Software 0 (0) (2023) 1–30. arXiv:https://doi.org/10.1080/10556788.2023.2246169, doi:10.1080/10556788.2023.2246169.
URL https://doi.org/10.1080/10556788.2023.2246169

[31] Quelle place pour le biométhane injectable en belgique? (2019).

[32] Asset study on technology pathways in decarbonisation scenarios. (2018).

[33] Technology data - generation of electricity and district heating (2016).

[34] Technology data - renewable fuels (2017).

[35] Technology data - energy storage (2018).

[36] G. I. Europe, Aggregated gas storage inventory (2021).
URL https://agsi.gie.eu/

[37] Fluxys, Fluxys belgium - tarifs de transport (2021).
URL https://www.fluxys.com/fr/natural-gas-and-biomethane/empowering-you/tariffs/tariff_fluxys-belgium-tra-2021

[38] Assessing the benefits of a pan-european hydrogen transmission network (2023).

[39] Analysing future demand, supply, and transport of hydrogen (2021).

[40] P. S. Matti Koivisto, Juan Gea-Bermúdez, North sea offshore grid development: combined optimisation of grid and generation investments towards 2050, IET Renewable Power Generation (2020).

[41] Electricity ten year statement 2015 - appendix E (technology) (2015).

[42] Elia, Load and load forecasts - total load (2023).
URL https://www.elia.be/en/grid-data/load-and-load-forecasts

[43] IEA, Tracking co2 capture and utilisation (2023).
URL https://www.iea.org/energy-system/carbon-capture-utilisation-and-storage#tracking

[44] E. U. E. information administration, Natural gas explained. factors affecting natural gas prices (2023).
URL https://www.eia.gov/energyexplained/natural-gas/factors-affecting-natural-gas-prices.php

[45] H. Consortium, The hydrogen for europe study (2022).
URL https://www.hydrogen4eu.com/_files/ugd/2c85cf_e934420068d44268aac2ef0d65a01a66.pdf

[46] Technology data - carbon capture, transport and storage (2021).

[47] J. Gea-Bermúdez, R. Bramstoft, M. Koivisto, L. Kitzing, A. Ramos, Going offshore or not: Where to generate hydrogen in future integrated energy systems?, Energy Policy 174 (2023) 113382.

[48] A. W. Solution, Desalination technologies and economics: Capex, opex & technological game changers to come (2016).
URL https://web.archive.org/web/20201123110805/https://www.cmimarseille.org/sites/default/files/newsite/library/files/en/1.6.%20C.%20Cosin_%20Desalination%20technologies%20and%20economics_%20capex,%20opex%20and%20technological%20game%20changers%20to%20come%20-ilovepdf-compressed.pdf

[49] E. H. Backbone, Estimated investment & cost (2024).
URL https://ehb.eu/page/estimated-investment-cost

[50] M. Berger, D.-C. Radu, K. Ryszka, D. Ernst, R. Fonteneau, G. Detienne, T. Deschuyteneer, The role of hydrogen in the dutch electricity system (2020).

Nomenclature

$\mathcal{C}, c$	set of clusters and cluster index
$\mathcal{E}, e$	set of hyperedges and hyperedge index
$\mathcal{G}$	hypergraph with node set $\mathcal{N}$ and edge set $\mathcal{E}$
$\mathcal{I}^n, i$	set of external variables at node n, and variable index
$\mathcal{N}, n$	set of nodes and node index
$\mathcal{T}, t$	set of time periods and time index
e_T, e_H	tail and head of hyperedge $e \in \mathcal{E}$
$\chi_i^n \in \mathbb{R}_+$	cost of the commodity i consumed by the node n
$\Delta_{i,+}^n \in [0,1]$	maximum ramp-up rate for flow i and conversion node n (frac. of capacity per unit time)
$\Delta_{i,-}^n \in [0,1]$	maximum ramp-down rate for flow i and conversion node n (frac. of capacity per unit time)
$\eta_+^n \in [0,1]$	charge efficiency of storage node n
$\eta_-^n \in [0,1]$	discharge efficiency of storage node n

$\eta_S^n \in [0,1]$	self-discharge rate of storage node n
$\iota_i^n \in \mathbb{R}_+$	cost related to the CO_2 captured from or released to the atmosphere by the node n
$\mu^n \in [0,1]$	minimum operating level of conversion node n (fraction of capacity)
$\overline{\kappa}^n \in \mathbb{R}_+$	maximum capacity of technology n
$\phi_i^n \in \mathbb{R}_+$	conversion factor between reference flow r and flow i for conversion node n
$\phi_{CO_2}^n \in \mathbb{R}_+$	conversion factor between carbon dioxide produced and flow i for conversion node n
$\pi_t^n \in [0,1]$	(operational) availability of conversion node n at time t
$\psi_r^n \in [0,1]$	percentage of the commodity r that need to be self-consumed in the node n for its operation
$\rho^n \in [0,1]$	charge-to-discharge ratio of storage node n
$\underline{\kappa}^n \in \mathbb{R}_+$	existing capacity of technology n
$E^n \in \mathbb{R}_+$	stock capacity of storage node n
$e_t^n \in \mathbb{R}_+$	inventory level of storage node n at time t
$K^n \in \mathbb{R}_+$	flow capacity of node n
$q_{it}^n \in \mathbb{R}_+$	flow of commodity i at node n and time t

Appendix

Parameters of technologies

n	Commodity r	$\underline{\kappa}^n$ GW or kt/h	$\bar{\kappa}^n$ GW or kt/h	κ^n_{tot} TWh/y or Mt/y	α^n -	μ^n -	Δ^n_+/Δ^n_- -	Source
PV	Electricity	0.0	50.0	-	0.0	0.0	-	[6]
WON		0.0	8.0	-	0.0	0.0	-	[6]
WOFF		0.0	9.0	-	0.0	0.0	-	[6]
NK		0.0	0.0	-	3.0/52.0	0.0	0.01/0.01	[33],[12]
FC		0.0	∞	-	0.0	0.0	1.0/1.0	[32],[33],[12]
CCGT		0.0	∞	-	2.0/52.0	0.4	1.0/1.0	[33],[12]
OCGT		0.0	∞	-	0.75/52.0	0.2	1.0/1.0	[33],[12]
EP	H_2	0.0	∞	-	2.0/365.0	0.05	1.0/1.0	[34],[12]
SMR		0.0	∞	-	0.0	0.0	1.0/1.0	[45], [12]
MT	CH_4	0.0	∞	-	0.0	0.0	0.01/0.01	[12]
BMT		0.0	$1.5 \cdot \kappa^n_{tot}$	14.08	10/365	0.5	0.01/0.01	[33], [31]
DAC	CO_2	0.0	∞	-	0.0	0.0	1.0/1.0	[46]
PCCC		0.0	∞	-	0.0	0.0	1.0/1.0	[12]
DU	H_2O	0.0	∞	-	0.0	1.0	0.0/0.0	[12]

Table 7: Technical parameters used for conversion nodes. The reference commodity for each nodes is given in the second column.

	Unit of r	ϕ_{el} GWh_{el}	ϕ_{H_2} GWh_{H_2}	ϕ_{CH_4} GWh_{CH_4}	ϕ_{CO_2} kt_{CO_2}	ϕ_{H_2O} kt_{H_2O}	ϕ_{fuel} GWh_{fuel} or kt_{fuel}	Source
NK	GWh_{el}	1.00	-	-	-	-	0.38	[33],[12]
FC			0.58	-	-	2.13	-	[32],[33],[12]
CCGT			-	0.6	2.97	-	-	[33],[12]
OCGT			-	0.45	2.23	-	-	[33],[12]
EP	GWh_{H_2}	0.74	1.00	-	-	3.70	-	[34],[12]
SMR		50.00		0.76	3.76	-	-	[45], [12]
MT	GWh_{CH_4}	-	0.98	1.00	4.95	-	-	[12]
BMT		16.67	-		4.95	-	0.33	[34], [31]
DAC	kt_{CO_2}	0.56	-	-	1.00	-	-	[46]
PCCC		2.42	-	-	0.90	-	-	[12]
DU	kt_{H_2O}	0.004	-	-	-	1.00	-	[12]

Table 8: Conversion factors for each conversion technology. These efficiencies are used in Eqs. (1). The sources for each efficiency are listed in the last column. The units of the reference commodity for each technology are in the second column while the values for the used conversion factors are given in the remaining columns. Note that only 90% of CO_2 can be captured by the PCCC from the CO_2 emitted by gas turbines (CCGT or OCGT). For electrolyser plants, the electricity used for compressing hydrogen is accounted for within the term ϕ_{el}.

n	$CAPEX^n$ M€/GW or M€/kt/h	θ_f^n M€/GW-yr or M€/(kt/h)-yr	θ_v^n €/MWh or €/t	χ_i^n €/MWh & €/t or €/t	L^n year	Source
PV	610.00	13.00	0.00	-	25	[32]
WON	943.00	12.00	0.18	-	25	[32]
WOFF	1995.00	32.00	0.39	-	25	[32]
NK	4700.00	105.00	7.8	1.69	50	[32]
FC	2668.00	40.00	1.04	-	20	[32]
OCGT	412.00	7.42	4.50	-	25	[33]
CCGT	750.00	15.00	1.73	-	30	[32]
EP onshore	333.33	6.67	0.00	-	35	[34]
EP offshore	502.13	6.67	0.00	-	35	[34], [9], [47]
SMR	805.00	37.80	0.17	-	25	[45]
MT	291.4	10.00	1.10	-	20	[32]
BMT	1733.00	165.18	0.00	10.23	15	[34], [31]
DAC	4000.00	20.00	0.00	-	30	[46]
PCCC	3150.0	0.00	0.00	-	20	[12]
DU	28.08	0.0	0.32	-	20.0	[48]

Table 9: Economic parameters used to model conversion nodes. CAPEX of offshore electrolysers considers the cost of the offshore platform on top of the cost of the technology.

	$\underline{\epsilon}^n$ GWh	$\bar{\epsilon}^n$ GWh	$\underline{\kappa}^n$ GW	$\bar{\kappa}^n$ GW	Source
PHP	5.3	5.3	1.3	1.3	[6]
CH_4S	8000	8000	7	7	Fluxys

Table 10: Capacity parameters used for storage nodes.

	η_S^n	η_+^n	η_-^n	ρ^n	ξ	ϕ_i^n $GWh_{elec}/GWh_{molecule}$	α^n	Source
Batteries	0.004	0.91	0.90	0.17	-	-	0.002	[35]
Pumped Hydro	0.0	0.89	0.89	1.0	-	-	0.00	[33]
H_2O storage	0.0	1.0	1.0	1.0	-	0.00036	0.00	[12]
H_2 storage	1.0	0.98	0.98	1.0	0.1	0.0	0.0	[12], [34]
CH_4 storage	1.0	0.99	0.99	0.5	-	-	0.0	[12]
CO_2 storage	1.0	1.0	1.0	1.0	0.2	-	0.0	[12]

Table 11: Technical parameters used for storage nodes.

	$\underline{\epsilon}^n$ GWh	$\bar{\epsilon}^n$ GWh	$\underline{\kappa}^n$ GW	$\bar{\kappa}^n$ GW	γ^n h	ω^n h	Source
Load shifting	1.5	1.5	1.5	1.5	0	-	[6]
Linepack	39.44	39.44	9.86	9.86	6	-	Fluxys
Load shedding 1h	-	-	0.128	0.2	0	1	[6]
Load shedding 2h	-	-	0.446	0.7	0	2	[6]
Load shedding 4h	-	-	0.534	0.607	0	4	[6]
Load shedding 8h	-	-	0.383	0.6	0	8	[6]
Load shedding 24h	-	-	0.191	0.3	0	24	[6]

Table 12: Technical parameters of flexibility nodes.

	CAPEX_{stock} M€/GWh or M€/kt	CAPEX_{flow} M€/GWh or M€/kt	ϑ_f^n M€/GW or M€/kt/h	θ_f^n M€/GW or M€/kt/h	ϑ_v^n M€/GWh or M€/kt	θ_v^n M€/GWh or M€/kt	L^n years	Source
Batteries	75.00	60.00	0.00	0.54	0.00	1.6e-3	25	[35]
Pumped Hydro	0.00	0.00	0.00	20.00	0.00	0.00	50	[32], [35]
H_2O storage	0.065	1.56	0.001	0.031	0.00	0.00	30	[12]
H_2 storage	8.40	0.00	0.55	0.00	0.00	0.00	30	[35]
CH_4 storage	0.10	0.00	0.003	0.00	0.00	0.00	80	[12]
CO_2 storage	0.10	0.00	0.00	0.00	0.00	0.00	20	[12]
Load shedding 1h	-	-	-	80	-	2.50	-	[6]
Load shedding 2h	-	-	-	80	-	2.00	-	[6]
Load shedding 4h	-	-	-	80	-	1.50	-	[6]
Load shedding 8h	-	-	-	80	-	1.00	-	[6]
Load shedding 24h	-	-	-	80	-	0.50	-	[6]

Table 13: Economic parameters used to model flexibility nodes (2050 estimates).

n	$\underline{\kappa}^n$ GW or kt/h	υ_t^n €/MWh or €/t	ϕ_{CO_2} $\text{GWh}_{CH_4}/\text{kt}_{CO_2}$	Source
NGNO	18.35	50.00 + 0.83	-	[36, 37]
NGUK	24.50	50.00 + 0.84	-	[36, 37]
NGFR	9.37	50.00 + 0.22	-	[36, 37]
NGDE	15.06	50.00 + 0.54	-	[36, 37]
SMI	26.81	164.80	4.95	[12]
H_2NL	25.65	75.00	-	[49]
CO_2E	3.50	2.00	-	[12]

Table 14: Economic and technical parameters used to model import or export nodes.

	$\underline{\kappa}^{n,WOFF}$ GW	$\underline{\kappa}^{n,WON}$ GW	$\underline{\kappa}^{n,PV}$ GW	$\underline{\kappa}^{n,NK}$ GW	$\underline{\kappa}^{n,HV}$ GW	length_{HV} km	β^n [-]	υ_t^n M€/GWh
Denmark	23.00	6.7	22.2	0.0	2	600	0.01	0.0448
United Kingdom	100.592	39.755	93.538	5.6	2.4	150	0.01	0.0447
Netherlands	60.137	9.676	94.856	0.0	5.4	50	0.01	0.0463
France	43.446	40.802	158.048	15.2	8.3	50	0.01	0.0475
Germany	52.199	68.376	268.215	0.0	1	50	0.01	0.046
Luxembourg	0.0	0.534	0.726	0.0	1	50	0.01	0.0399

Table 15: Technical and economical parameters used to model the electricity import from neighbouring countries.

	$\underline{\kappa}^n$ GW	$\bar{\kappa}^n$ GW	length km	ϕ_i^n	ϕ_l^n $GW_{el}/GW_{molecule}$	Source
Submarine HVAC	2.3	100	-	0.93	-	[6], [50]
Inland HVAC	3	100	-	0.93	-	[6]
Submarine HVDC	0	100	40	0.98	-	
Submarine H_2 pipeline	0	100	40	0.9992	0.015	
Inland H_2 pipeline	0	100	47	0.9992	0.015	
Inland natural gas pipeline	60.5	100	47	0.9992	-	

Table 16: Technical parameters of transmission nodes.

	length km	CAPEX M€/GW	θ_f^n M€/GW	θ_v^n M€/GWh	lifetime year	Source
Submarine HVAC	40	4.57 * length + 217.2	6.00	1.00e-6	70	[6], [12]
Inland HVAC	47	133.33	2.00	1.00e-6	70	[6], [12]
Submarine HVDC	40	1 * length + 762.6	0.015 * CAPEX	1.00e-6	40	[6]
Submarine H_2 pipeline	40	0.227 * length	0.03 * CAPEX	1.00e-6	40	[1]
Inland H_2 pipeline	47	0.227 * length	0.03 * CAPEX	1.00e-6	40	[1]
Inland natural gas pipeline	47	0.0925 * length	0.03 * CAPEX	1.00e-6	40	[12]

Table 17: Economic parameters of transmission nodes.

Results of High Renewable Scenario

	Total production (TWh)	Curtailment (TWh)	Capacity factor (%)	Usage factor (%)	Hours of curtailment
Photovoltaic Panels	29.18	0.17	11.72	99.43	152
Offshore Wind Turbines	31.86	1.78	39.11	94.71	566
Onshore Wind turbines	39.75	1.85	22.14	95.55	596

Table 18: Total productions and curtailments of renewable technologies.

	K_f^n (GW)	Total $q_{i_f,t}^n$ (TWh)	Total $q_{i_r,t}^n$ (TWh)
HV lines OFF - COA	5.87	24.36	0.01
HV lines COA - INL	5.66	21.20	3.21
H_2 pipelines OFF - COA	1.57	5.49	0.00
H_2 pipelines COA - INL	4.90	12.38	0.00
CH_4 pipelines COA - INL	60.50	74.37	0.00

Table 19: Capacities in the forward direction, K_f^n, annual amount of the flow in the forward direction, Total $q_{i_f,t}^n$, and annual of the energy flow in the reverse direction, Total $q_{i_r,t}^n$, of each transmission node installed for **Scenario 2**.

	E^n (GWh or kt)	K^n (GW or kt/h)	Peak q_i^n (GW or kt/h)	Peak q_j^n (GW or kt/h)	# cycles
OFF Batteries	1.96	-	-	-	128.10
(Charge)	-	0.13	-	0.13	-
(Discharge)	-	0.76	0.76	-	
COA Batteries	14.41	-	-	-	129.78
(Charge)	-	1.00	-	1.00	-
(Discharge)	-	6.03	5.62	-	
INL Batteries	23.83	-	-	-	146.00
(Charge)	-	1.38	-	1.38	-
(Discharge)	-	8.26	8.26	-	
OFF H_2O storage	238.26	0.25	0.25	0.15	3.22

Table 20: Stock capacities, E^n, flow capacities, K^n, peak discharge, Peak q_i^n, peak charge, Peak q_j^n and number of cycles of each storage technologies installed in the optimal solution for **Scenario 2**.

	Preinstalled capacity κ^n (GW or kt/h)	Total energy q_i^n (TWh or Mt)	Peak power q_i^n (GW or kt/h)
Elec Denmark	2.00	0.74	0.38
Elec United Kingdom	2.40	4.75	2.40
Elec Luxembourg	1.00	4.26e-3	0.01
Elec France	8.30	5.53	5.40
Elec Netherlands	5.40	1.56	1.00
Elec Germany	1.00	2.54	1.00
INL H_2 Netherlands	25.65	65.03	12.07
COA NG Norway	18.35	0.00	0.00
COA NG United Kingdom	24.50	0.00	0.00
COA NG France	9.37	74.43	9.37
COA SG North Africa	26.81	0.00	0.00
INL NG Germany	15.06	11.81	15.06
INL CO_2	3.50	17.41	2.25

Table 21: Flow capacities, κ^n, annual energy imported or exported, Total q_i^n and peak energy imported or exported of each import and export nodes and neighbouring country clusters for **Scenario 2**.

	K^n (GW)	Total q_i^n (GWh)	# hours
Load shifting	1.500	11.24	36
Load shedding 1h	0.128	0.256	2
Load shedding 2h	0.446	1.784	4
Load shedding 4h	0.534	4.3	10
Load shedding 8h	0.383	8.43	23
Load shedding 24h	0.300	28.3	70
Energy not served electricity	5.25	39.03	16
Energy not served hydrogen	0.000	0.000	0
Energy not served natural gas	0.000	0.000	0

Table 22: Flow capacities or max energy not served, K^n, annual load reduction, Total q_i^n and number of hours of each flexibility nodes reduce the load or the energy is not served for **Scenario 2**.

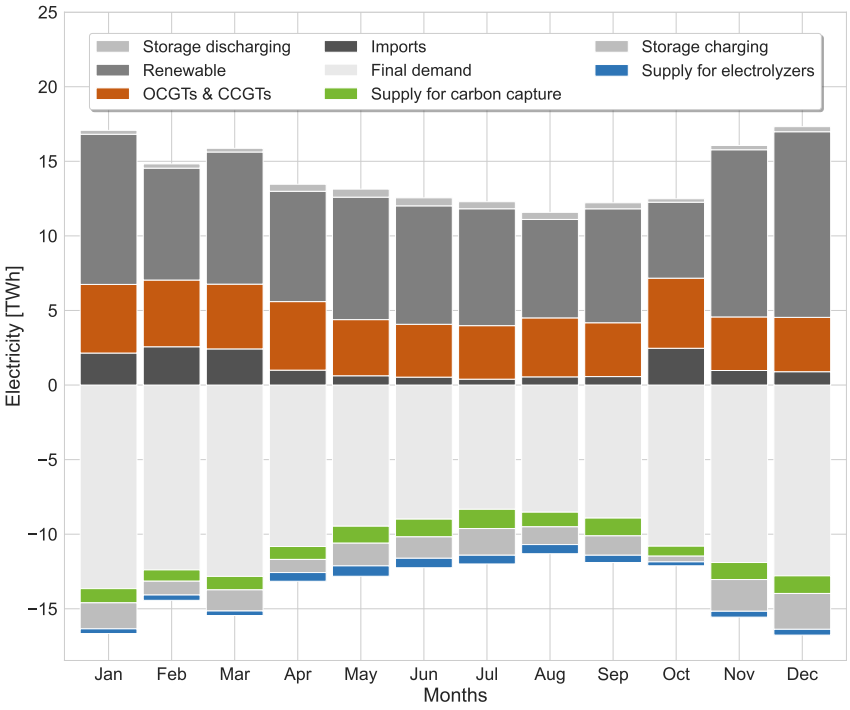

Figure 16: Electricity balance of the entire system for each month of the year for **Scenario 2**.

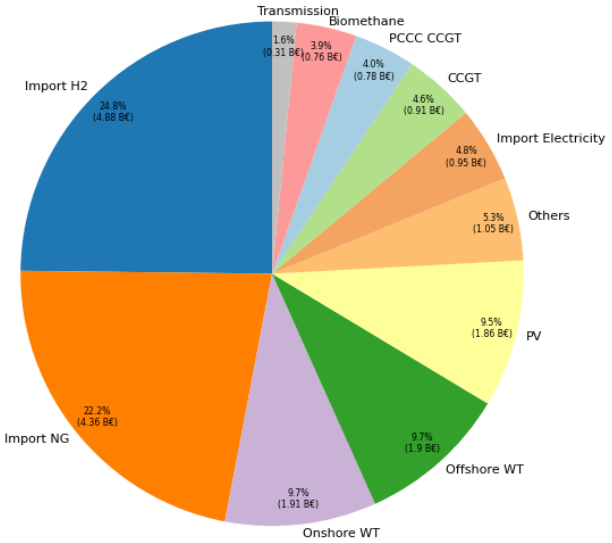

Figure 17: Costs of each node and neighbour clusters for **Scenario 2**.